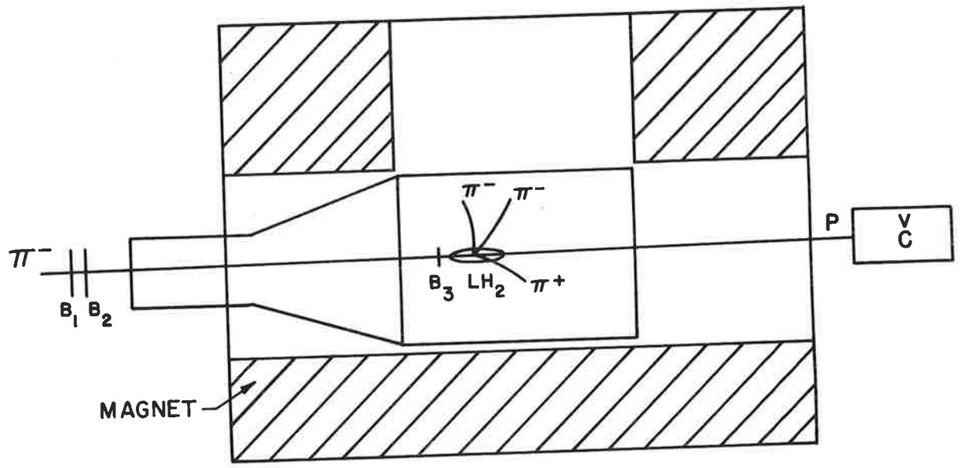

Fig. 7. Side view of the facility

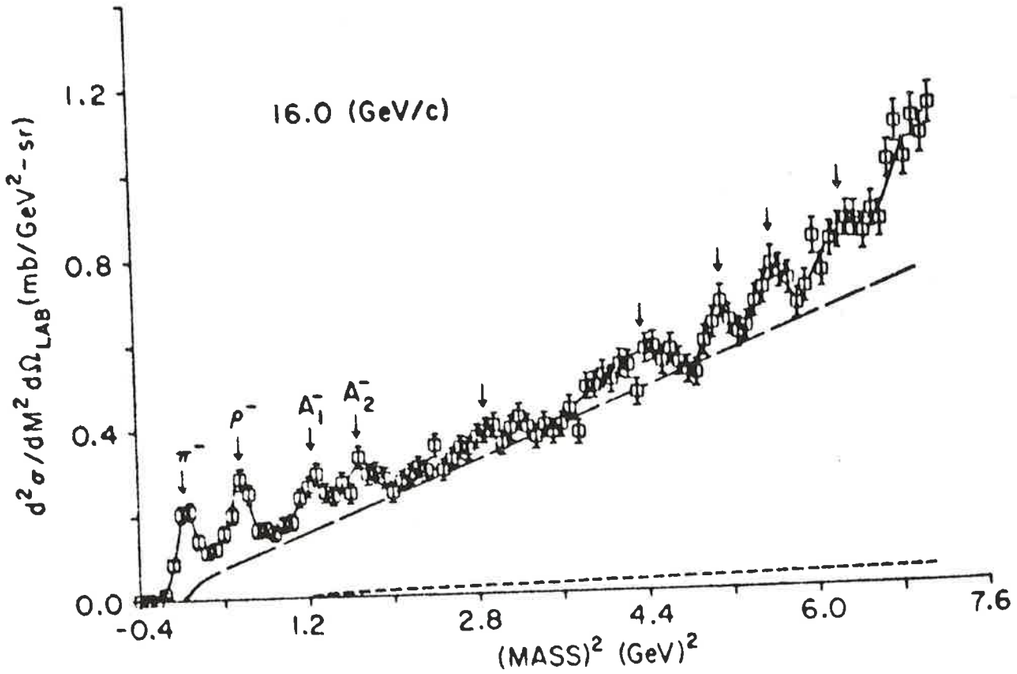

Fig. 8. Missing mass data from Anderson et al.,[4] from backward production

π EXCHANGE*

Geoffrey Fox
California Institute of Technology,
Pasadena, California 91109

ABSTRACT

The study of π-exchange processes can be naturally divided into three regions corresponding to $-t \simeq m_\pi^2$, 0.6, and $\gtrsim 1$ $(GeV/c)^2$ respectively. In the first (which corresponds to the long-range force with impact parameter $b \gtrsim 1/m_\pi \simeq 1.4$ fm) we show that the zero parameter Poor Man's absorption model is in splendid agreement with experiment. Further we discuss the validity of current and future π-π and K-π scattering analyses. In the second region ($b \simeq 1$ fm), we contrast the systematics of single vector meson production ($\pi N \to (\rho,\omega)N$, $KN \to K^*N$) with those of πN CEX, $\pi N \to \eta N$, and KN CEX. Better data on $\pi^- p \to \rho^o n$ is needed for unambiguous results, but the two sets of data show a pleasing similarity. In the large $-t \gtrsim 1$ $(GeV/c)^2$ region ($b \simeq 0 \to 0.5$ fm), there is a striking similarity around 5 GeV/c between photoproduction and strong interaction π exchange processes. The former--in contrast to the shrinkage of ρ exchange $\pi^- p \to \pi^o n$ --show a universal $p_{lab}^{-2}\, e^{3t}$ behavior. New strong interaction experiments in both π and ρ (A_2, K^{**}) exchange reactions, for $-t \gtrsim 1$ $(GeV/c)^2$ and $p_{lab} \gtrsim 10$ GeV/c are needed to confirm or deny the universality and hence importance of this new component of scattering.

*Work supported in part by the U.S. Atomic Energy Commission under Contract AT(11-1)-68. This paper also known as CALT-68-335.

INTRODUCTION

(i) Apologia

Originally I was asked to talk on resonance production mechanisms with, implicitly, a contract to study their relation to meson spectroscopy. Unfortunately, on reflection, I was unable to detect any significant overlap between the two fields. This unusually neat division between two branches of physics, followed because details of production mechanisms have only been studied for the clean low-lying resonances, e.g., Δ^{++}, ρ, $Y^*(1385)$, ...; these joys for spectroscopists of former years are now but played out elder statesmen and no longer of spectroscopic interest. Given an unencumbered desire to study differential cross-sections and density matrix elements for resonances, one might discuss:

(a) Diffraction production of real (e.g., $N^*(1688)$) and mythical (e.g., A_1) particles.

(b) Tests of the quark (SU_6) model[1] which, of course, relates Δ to p, and ρ to π and so involves resonance reactions. Here there are many strikingly successful predictions for decay density matrix elements and double correlations in, for instance, $\pi N \to \pi\Delta$ and $\pi N \to \rho\Delta$. Further, some quite interesting theoretical developments in dual models have occurred in this field.

(c) Tests of high-energy models, e.g., cuts, poles, absorption, etc. Here one can make a further division: first, consider those reactions that go by (mainly) natural parity exchange, e.g., $\pi N \to \pi\Delta$, $K^{\pm}p \to K^{*\pm}p$, and $\pi^+p \to \rho^+p$ + $\pi^-p \to \rho^-p$ $\ominus$ $\pi^-p \to \rho^0n$ ($\simeq$ ω-exchange only). These have

qualtitatively similar behavior to the related stable particle data (e.g., $\pi^-p \to \pi^0n$ and $\pi^+p \to \pi^0\Delta^{++}$ both have a dip at $t \simeq -.6$ $(GeV/c)^2$) and, with present statistics, have given little fresh information. More interesting are the π-exchange reactions: here resonance data is our main source of information and so play a unique role. In deciding on a topic for this talk, I found that I knew little about (a), had reviewed (b) rather recently[2] and so we are left with π-exchange, which was also considered in Ref. 2 but only incoherently.

(ii) π-Exchange

The study of π-exchange processes can be naturally divided into the three regions marked in Fig. 1. The first, discussed in Section A, is unique to π-exchange as it corresponds to the region, $-t$ of $O(m_\pi^2)$, governed by the long-range (π-pole) force. In the impact parameter (b) plane this is $b \gtrsim 1/m_\pi = 1.4$ fm which is also marked in Fig. 1. Remember that Fourier-Bessel transforms are defined as

$$f(s,b) = 1/(32\pi\sqrt{s}\, q\, b^n) \int_0^\infty H(s,t)\, J_n(b\sqrt{t})\, d(-t) \qquad (1)$$

in terms of the usual (s-channel) helicity amplitudes $H(s,t)$. In (1) $n = |\lambda_1 - \lambda_2 - \lambda_3 + \lambda_4|$ is, as usual, the net s-channel helicity flip. λ_i are the individual particle helicities and in (1) we have removed a kinematic zero b^n. b and t are conjugate variables: the correspondence for the three regions in Fig. 1 is only qualitative.

The small $-t$, large b region A is superficially a success for the strong absorption model (SCRAM)[3]. However, a closer look suggests that there is an entirely different explanation: this lies in the Poor Man's

Absorption (PMA) model which postulates smooth extrapolation from $t = m_\pi^2$ to $t=0$. The latter model, which has no free parameters, gives a good description of all the current small $-t$ π-exchange data. The new Argonne np CEX data[4] showed that the old experiment[5] had a factor of two error in normalization: this renormalization has removed the one embarrassing failure of the PMA model. Further, in this section, we delimit the regions of both t and lab momentum that are necessary for successful π-π and K-π scattering analyses. This might even be considered relevant for meson spectroscopy as one way of quantitatively studying low-spin high-mass meson resonances (e.g., S and P wave resonances in the f^o region) is by π-π phase shift analysis.

In Section B we study the region $t \simeq -.6$, $b \simeq 1$ fm and contrast the systematics of ρ_{oo} $d\sigma/dt$, for vector meson production, $[\pi N \to \rho N$, $\pi N \to \omega N$ and $K,\bar{K}N \to K,\bar{K}^* N]$ with those of $d\sigma/dt$ of the well-known quartet πN CEX, $\pi N \to \eta N$ and $\overset{(-)}{K}N$ CEX. Current "theories"[2,3,6,7] that explain the latter data give distinctly different predictions for the vector meson processes. The two sets of reactions show an encouraging similarity, but we need better data on $\pi^- p \to \rho^o n$ to allow an unambiguous distinction between the various models.

Finally, in Section C we study the large $-t > 1$ $(GeV/c)^2$ and small $b \simeq 0$ to 0.5 fm region. First, we remind the reader of the universal $p_{lab}^{-2}\ e^{3t}$ behavior observed[8] for current photoproduction data in this $-t$ region. Let us suppose this is no accident but rather represents a new and fundamental interaction. Then it is important to check for its occurrence in purely hadronic reactions. Many of the photoproduction processes are

π-exchange dominated. These show, around 5 GeV/c and $-t > 1$ $(GeV/c)^2$, a striking similarity to strong-interaction π-exchange reactions, in both the size and the shape of the differential cross-section. It is difficult to make this comparison complete because of a striking experimental bias. Virtually all exchange data in <u>strong interactions</u> for $-t \geq 1$ $(GeV/c)^2$ has $p_{lab} \lesssim 5$ GeV/c and here it shows dips ($\pi N \to \eta N$) and Regge energy dependence (faster than p_{lab}^{-2}). In contrast, nearly all the <u>photoproduction</u> data for this t region lies in the range $5 \lesssim p_{lab} \lesssim 18$ GeV/c , and shows the quite different $e^{3t}\ p_{lab}^{-2}$ behavior. We examine the few exceptions to this bias. However, new strong interaction data for $-t \gtrsim 1$ $(GeV/c)^2$ and $p_{lab} \gtrsim 10$ GeV/c are really needed to establish or deny a difference from photoproduction. In conclusion, we note the numerical coincidence between e^{3t} and both the Holy Trinity and the $e^{-3p_\perp^2}$ dependence of inclusive reactions.

A. SMALL t, LARGE IMPACT PARAMETER BEHAVIOR

The behavior of π-exchange reactions in this region (marked A in Fig. 1) can be both systematized experimentally and understood theoretically by a division into three classes--classified by the small t behavior of their Feynman diagram Born terms.

(I) <u>Crippled π</u>: <u>Born Term $= g_I t/(t-m_\pi^2)$</u>

Examples are $p\bar{p} \to n\bar{n}$, $np \to pn$, $\gamma p \to \pi^+ n$, $\gamma n \to \pi^- p$, $2\rho_{11}^H\ d\sigma/dt$ ($\pi^- p \to \rho^o n$, $K^- p \to \bar{K}^{*o} n$, $\pi^- p \to f^o n$, etc.) (2/I)

(II) Half-Asleep π: Born Term = $g_{II}\sqrt{-t}/(t-m_\pi^2)$

Examples are ρ^H_{oo} $d\sigma/dt$ ($\pi^- p \to \rho^o n$, etc.), $pp \to n\Delta^{++}$, $\gamma p \to \pi^- \Delta^{++}$, $\gamma p \to \omega p$. (2/II)

(III) Fully-Fledged π: Born Term = $g_{III}/(t-m_\pi^2)$

Examples are $p\bar{p} \to \Delta\bar{\Delta}$, $\pi^+ p \to \rho^o \Delta^{++}$, $\pi^+ p \to f^o \Delta^{++}$, etc. (2/III)

Now divide any amplitude into three pieces:

$$A(t) = A_\pi^{LOW}(t) + A_\pi^{HIGH}(t) + A_{other}(t) \quad . \tag{3}$$

A_π^{LOW}, A_π^{HIGH} are the contributions to π-exchange coming from low $b \leq b_o$ and high $b \geq b_o$ partial waves. Here b_o may be conveniently chosen as:

$$b_o = \frac{1}{m_\pi} \simeq 7\ (GeV/c)^{-1} = 1.4\ fm \quad . \tag{4}$$

$A_{other}(t)$ is the contribution of everything else except π-exchange. A_{other} is dominated by waves for $b < b_o$ whereas A_π^{HIGH} is 60% for Class III and 80% for Class II of the total Born term at t=0.

All theories agree that $A_\pi^{HIGH}(t)$ exists, and is essentially unaffected by absorption[11] and other dynamical myths--it is given uniquely by the residue of the nearly π pole. The total amplitude A(t) is determined by the relative sizes of the sacrosanct piece $A_\pi^{HIGH}(t)$, $A_\pi^{LOW}(t)$, and $A_{other}(t)$.

Class III: Fully-Fledged π

A^{HIGH} ($t \simeq 0$) is enormous for the fully-fledged π--at least in the examples quoted in (2/III). This is graphically illustrated in Fig. 2(a) which compares $\pi^+ p \to \rho^o \Delta^{++}$ and $\pi^+ p \to \omega^o \Delta^{++}$. The latter is essentially an upper bound on $A_{other}(t)$ for the $\rho^o \Delta^{++}$ reaction where "other" = A_2. Thus, from exchange degeneracy (EXD), the A_2 exchange in $\rho^o \Delta^{++}$ = the ρ exchange in $\omega^o \Delta^{++}$ at t=0 and the latter will be less than the total $d\sigma/dt$ for $\omega^o \Delta^{++}$ which has as well substantial B exchange.

Class II: Half-Asleep π

$A_\pi^{HIGH}(t)$ also dominates over $A_{other}(t)$ in the half-asleep class II. Indeed, at a given t-value the ratio $|A_\pi^{HIGH}(t)/A_{other}(t)|$ is similar in the two classes II and III. This is indicated experimentally in Fig. 2(b) which compares $\pi^- p \to \rho^o n$ with $\pi^+ n \to \omega^o p$. The latter is again bound on the A_2 contribution to $\rho^o n$. Note that the $\rho^o n$ and $\omega^o p$ differential cross-sections cross at the same t-value ($t \simeq -.25\ (GeV/c)^2$) as do the $\rho^o \Delta^{++}$ and $\omega^o \Delta^{++}$ reactions. Further, the ratio $\rho^o n/\omega^o p$ at $t \simeq -m_\pi^2$ is around 20--the same value as for $\rho^o \Delta^{++}/\omega^o \Delta^{++}$ at this t. Theoretically EXD predicts[9,10] that the ratio $|A(\rho)/A(\omega)|^2$ should be the same in the single and double resonance reactions and be $\cot^2 \pi\alpha_\pi/2$ for π v. B and $\cot^2 \pi\alpha_{A_2}$ for A_2 relative to ρ exchange. The data in Fig. 2 suggest that the ω reactions are rather bigger than this prediction--a deviation which is currently "explained" as a breaking of EXD. However, it is sufficient here to note that the similar ρ/ω ratios in the Class II and III reactions is not unexpected theoretically.

In spite of this ratio similarity, it is clear from Fig. 2 that one

can only realize the full vitality of the π in the fully-fledged reactions. Thus in the half-asleep Class II, the π is obscured for $0 \leq -t \lesssim m_\pi^2$ as its amplitude, exhibited in Eq.(2/II), vanishes at t=0 due to the $\sqrt{-t}$ factor in the Feynman Born term: in this region measured half-asleep cross-sections are obscured by <u>different</u> amplitudes: those that are non-vanishing at t=0. For instance, in $\pi N \to \rho N$, $2\rho_{11}^H$ $d\sigma/dt$ takes over in this t region [cf. Fig. 4]. However, in Class III there is no such difficulty and the cross-section rises until at t=0 it is a splendid factor of 200 above background. We can draw two qualitative conclusions from this discussion. First we consider meson-meson scattering and then go on to discuss the relevance to high-energy exchange models.

<u>π-π and K-π Scattering</u>

Studies of π-π and K-π scattering will always be unsatisfactory in the half-asleep processes, e.g., $\pi^- p \to \pi^+\pi^- n$ and $K^- p \to K^-\pi^+ n$. Thus Fig. 2(b) shows that the background is at best ($t \simeq -m_\pi^2$) 5% in cross-section or 20% in amplitude. The situation in published[12] π-π (K-π) analyses is much worse as they use data in typically $0 \leq -t \leq .2$ or $.5\ (\mathrm{GeV/c})^2$; here Fig. 2(b) shows the background to be even bigger. In principle, Fig. 2(a) shows that the Δ^{++} reactions ($\pi^+ p \to (\pi^+\pi^-)\Delta^{++}$, $K^+ p \to (K^+\pi^-)\Delta^{++}$) are much more satisfactory--at t=0 the background is negligible. However the effect of the kinematic cut-off in t implies that high incident energies are needed to realize this advantage. For instance, in $\pi^+ p \to (\pi^+\pi^-)\Delta^{++}$, the minimum allowed value of -t is given by

$$-t_{lim} \simeq (m^2 - m_\pi^2)(m_\Delta^2 - m_N^2)/(2m_N\, p_{lab}) \qquad (5)$$

where m is the mass of the $\pi^+\pi^-$ system. The fully-fledged π vitality will

be realized if $-t_{lim} \leq 1/2\ m_\pi^2$ which requires $p_{lab} = 20$ GeV/c for $m^2 = m_\rho^2$ and $p_{lab} = 50$ for the f^o. Current work on π-π scattering, using the Δ^{++} reactions, has, of necessity, not used these lab momenta and correspondingly are no more reliable than the half-asleep analyses. In the latter the kinematic t limit is much more favorable. In $\pi^- p \to \pi^+\pi^- n$ we have:

$$-t_{lim} \simeq (m^2 - m_\pi^2)^2/(4p_{lab}^2) \quad . \qquad (6)$$

From Fig. 2(b) we might estimate that the range $1/2\ m_\pi^2 \leq -t \leq .1\ (\mathrm{GeV/c})^2$ was the best compromise for studying π-π scattering in the unfortunate half-asleep environment. This requires $p_{lab} > 3$, 8, and 14 GeV/c for the study of the ρ, f, and g mesons, respectively.

We deduce that at current accelerators, the half-asleep reactions will probably give the most reliable answers for meson-meson scattering. At NAL, however, the fully-fledged Δ^{++} reactions will show their full beauty and take over--at least in the lower π-π mass regions--from their poor cousin, those maligned half-asleep processes.

<u>Class I: Crippled π</u>

Although there was difficulty with detailed studies of meson-meson scattering, the large size of $A_\pi^{HIGH}(t\simeq 0)$ --a quantity we agreed was unaffected by absorption, etc.--implies that all models give the same predictions for the qualitative behavior of Class II and III reactions near t=0. Dynamics is only important at t≃0 for π-exchange in the crippled class (I) and we now turn to this. It is clear from Eq.(2) that $A_\pi^{HIGH}(t)$

has an identical t-dependence for Classes I and III. They only differ in their overall normalization which is determined by the relative size of g_I and g_{III} in (2/I) and (2/III), i.e., by the size of the π pole coupling constants. In the quoted examples, the amplitude $A_\pi^{HIGH}(t)$ is a full order of magnitude smaller for Class I compared with Class III. It follows that Class I cross-sections near t=0 are much more sensitive to the details of the low partial waves: $A_\pi^{LOW}(t)$ and $A_{other}(t)$. Write for -t of $O(m_\pi^2)$,

$$N = \frac{g_I\, t}{(t-m_\pi^2)} + C_1 \quad . \tag{7}$$

Here N is the s-channel nonflip amplitude containing the π pole.

Then in the Born term: $C_1 = 0$ and the cross-section vanishes at t=0 in complete disagreement with experiment. In the Poor Man's Absorption Model (PMA) we put $C_1 = -g_I + C_2$ giving

$$N = \frac{g_I\, m_\pi^2}{(t-m_\pi^2)} + C_2 \tag{8}$$

and assume C_2 small. In the t-plane this corresponds to the (reasonable) assumption of a smooth extrapolation of the π pole from $t = m_\pi^2$ to $t\simeq 0$. In the b-plane, it corresponds, for f(b), defined in Eq.(1), to the nondescript behavior

not the change of sign

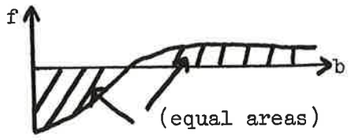

of the Born term. The PMA model gives <u>absolute</u> predictions for <u>all</u> crippled

π cross-sections at t=0.

In units of $mb/(GeV/c)^2$, some examples are:

$$\gamma p \to n\pi^+ \ , \ \gamma n \to p\pi^- \ : \ d\sigma/dt = 3.01 \times 10^{-3}\ (p_{lab}/5)^{-2}$$

$$np \to pn \ , \ p\bar{p} \to n\bar{n} \ : \ d\sigma/dt = 5.8\ (p_{lab}/5)^{-2}$$

$$\pi^- p \to \rho^o n \ : \ 2\rho_{11}^H\, d\sigma/dt = 1.48\ (p_{lab}/5)^{-2} \quad . \tag{9}$$

This is compared with experiment in Fig. 3 in which various crippled π cross-sections are plotted in a normalization such that PMA would predict 1 at t=0. This simple model is in amazing agreement with experiment.

The <u>absorption model</u>[2,3,13] gives similar predictions for C_1 but:

(i) One needs a <u>strong cut</u> (SCRAM) corresponding to the usual S-wave absorption constant $C \simeq 1.3$. This leads to the implausible snake-like

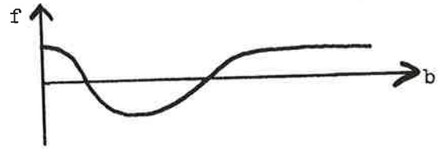

for the partial wave amplitude f(b).

(ii) Philosophically the PMA prediction at t=0 seems prettier as it depends only on a simple extrapolation in t through m_π^2. Such an extrapolation has proved very successful in the application of PCAC. In SCRAM, the value of $d\sigma/dt$ at t=0 comes solely from the cut whose amplitude can be written symbolically as $\lambda(\text{fudge factor}) \circledast \int_0^\infty \text{WEIGHT}(t')\ \text{BORN}_\pi(t')\ d(-t')$. The resultant $d\sigma/dt$ (t=0) is a complicated combination of two parameters, namely $\lambda \simeq 2$ (or equivalently C), and the t'-dependence of the input π (Regge) pole ($\text{BORN}_\pi(t')$). The final simplicity of Fig. 3--predicted without any

parameters by PMA--is a fluke in SCRAM.

(iii) Further, the necessary parameters--i.e., $\lambda \simeq 2$--give completely wrong results when applied to the real parts of ρ and A_2 exchange in $\pi^- p \to \pi^o n$ and $\pi^- p \to \eta n$, etc. Again, calculations[2] at 5 GeV/c reveal that the low partial waves of Reggeized (crippled) π-exchange are no bigger than those for ρ and A_2 exchange. So there is no special reason to absorb π-exchange and not ρ and A_2. It follows that the explanation of crippled π-exchange in terms of the absorption model lacks conviction. Why should we use it for the π when it fails for the ρ and A_2?

Interpreting the PMA model in the j-plane leads to a complicated structure. Considering just nonflip and single flip vertices, the PMA model may be decomposed into precisely three "trajectories". These consist of two $\tau P-$ exchanges--one M=0 and one M=1, plus one $\tau P+$, M = 1 trajectory. (M is the Toller quantum number[14].) Conversely, the experimental data on Classes I to III show this (i.e., three) is the minimum number of trajectories one must use, in a pole only model, to describe π-exchange data of Classes I to III for region A. In fact, for instance, $\pi^+ p \to f^o \Delta^{++}$, $\gamma p \to \rho^- \Delta^{++}$ and $\bar{p} p \to (\overline{\Delta^{++}})\Delta^{++}$ have components that do not fall into any of the classes I to III: in the PMA model, these correspond to extra "poles" with M=2 quantum numbers and make the j-plane interpretation even more unsavory. There is no conclusive evidence for or against M=2 exchange in high-energy physics: confirmation or denial of its existence would be very important. For instance, quark models[2] predict only M=0 or 1 as they relate all scattering amplitudes to a $1/2^+ 1/2^+ \to 1/2^+ 1/2^+$ "black box": this cannot have M=2 exchange[15].

We finish with some disconnected remarks on PMA and its relation to other models of π-exchange.

(a) PMA is consistent with vector dominance (VDM). Indeed, the success of the Cho-Sakurai[16] model may be interpreted not as a success for VDM but rather as a success of PMA. In the more general Jackson-Quigg pseudomodel[17], PMA follows from the dominance of the π FESR by the nucleon Born term.

(b) PMA is consistent with the coherent droplet model[18]--it corresponds to a particular form near t=0 of the droplet.

(c) In $\pi^- p \to \rho^o n$, PMA specifies the amplitude structure near t=0 and hence all the density matrix elements of the ρ. The excellent agreement of this with experiment[19] is demonstrated in Fig. 4. Indeed, the absorption model of Williams[20], used by Leith[19], is precisely the PMA model specialized to $\pi^- p \to \rho^o n$. PMA also predicts the small t density matrix elements for all $\pi\pi$ masses. For instance, for $\pi^- p \to (\pi\pi)n$,

$$2\rho^H_{11}/\rho^H_{oo} \simeq 2(m_\pi^2/-t)(m_\pi/m_{\pi\pi})^2 \, \varepsilon_L \qquad (10)$$

where $\varepsilon_L = 0$, 1, and 3 for S, P, and D $\pi\pi$ waves, respectively[21]. Note that the "absorption" corrections decrease with increasing mass $(1/m^2_{\pi\pi})$ but increase with increasing angular momentum L. These predictions are, I believe, unchecked at present. The PMA model should be useful in π-π and K-π phase shift analyses--especially in understanding some of the background[22] in the difficult half-asleep processes $\pi^- p \to (\pi^+\pi^-)n$ and $K^- p \to (K^-\pi^+)n$, discussed earlier in this section.

(d) In $\gamma p \to \pi^- \Delta^{++}$, PMA coincides with the gauge invariant Born term (just as it did for $\gamma p \to \pi^+ n$). Analogously to Eq.(10) we write[23]

$(\gamma p \to \pi^- \Delta^{++})$ crippled π part/$(\gamma p \to \pi^- \Delta^{++})$ half-asleep part $\simeq$

$$\simeq 2\left[m_\pi^2/-t\right]\left[m_\Delta m_\pi/(m_\Delta^2 - m_N^2)\right]^2 \qquad (11)$$

which predicts the (non-zero) cross-section at t=0 in agreement with experiment. (Ref. 8, Fig. 30.)

(e) The behavior of the curves in Fig. 3 away from t=0 are of some dynamical interest. (i) $np \to pn$ has a sharper t-dependence than $p\bar{p} \to n\bar{n}$, $\gamma n \to p\pi^-$ is sharper than $\gamma p \to n\pi^+$. This is "explained" by the interference of ρ-exchange, which (approximately) vanishes at t=0 with the PMA π-exchange. The data imply a relative sign of π and ρ exchange in agreement with the quark model[2,24]. (ii) The very sharp $\pi^- p \to \rho^0 n$ forward peak is incomprehensible. I would have expected it to lie somewhere between $np \to pn$ and $p\bar{p} \to n\bar{n}$. The current data[19] has quite large errors--it is important to confirm this surprising feature. (iii) Photoproduction after the natural PMA normalization at t=0 is notably bigger at large -t than the strong interaction data shown. (Compare $\gamma p \to n\pi^+$ with $p\bar{p} \to n\bar{n}$; $\gamma n \to p\pi^-$ with $np \to pn$.) This may reflect some basic dynamical difference between photoproduction and strong interactions (e.g., fixed poles in the former)--see Section C.

(f) The argument in (e)(i) is the only unambiguous separation of ρ (A_2) exchange from the natural parity component of π-exchange generated by PMA. In principle they can be separated by their energy dependence ($\alpha_\rho(0) - \alpha_\pi(0) \simeq 0.5$) but present data are over too small an energy range for this to work. Indirect arguments (e.g., use SU_3/EXD on ω-exchange in $\gamma p \to \pi^0 p$, $\pi^\pm p \to \rho^\pm p$) and explicit fits suggest ρ, A_2 exchange will

be sizeable for $-t \simeq 0.5$ (GeV/c)^2. This is only accurate to a factor of two; correspondingly it is not obvious whether the much-debated (lack of) dip at $t \simeq -0.6$ (GeV/c)^2 in $\pi^+ p \to \omega^0 \Delta^{++}$, $\pi^- p \to \omega n$, and $\gamma p \to \eta n$ is[3,6,7] due to PMA $\pi(B)$ corrections or lack of WSNZ in ρ-exchange.

In conclusion, the simple PMA model gives an excellent description of π-exchange for small -t. It is important to check it in other reactions, e.g., angular decay of $\pi^- p \to f^0 n$ and $np \to pn$ at NAL energies. In the latter case, ρ and A_2 contributions to $A_{other}(t\simeq 0)$ may swallow up dull old PMA.

B. $-t \simeq 0.6$ (GeV/c)^2, b $\simeq$ 1 fermi

In this section we will discuss the current experimental situation for the zero systematics of pure unnatural parity exchange amplitudes. To isolate unnatural parity exchange, one can look at reactions of the type

$$\pi N \to (\pi\pi)_{S\text{-wave}} N : d\sigma/dt \qquad (12a)$$

$$\pi N \to \rho N : \rho_{oo}\, d\sigma/dt \qquad (12b)$$

$$\pi N \to (\pi\pi)_{S\text{-wave}} \Delta : d\sigma/dt \qquad (12c)$$

$$\pi N \to \rho \Delta : \rho_{oo}\, d\sigma/dt \qquad (12d)$$

(and their SU_3 friends)

The reactions involving Δ's are complicated: $\rho_{oo}\, d\sigma/dt$ being a mixture of n = 0, 1, and 2 in the s-channel. We do not expect any particular dip structure, unless one of these n values dominates. The recent report of a dip at $t \simeq -0.75$ (GeV/c)^2 in $\pi^+ p \to \rho^0 \Delta^{++}$ at 3.7 GeV/c [25] is not

confirmed by data at 5.45 GeV/c [26]. It would be exciting to see this re-examined with higher statistics and consideration of the double correlations to find the Δ^{++} spin structure. Here, in view of the limited statistics of the current experiments and the complication of the theory, I will ignore Δ production. Again, there is no relevant $(\pi\pi)_{S\text{-wave}}$ data of which I am aware. So I will discuss the reaction $\pi N \to \rho N$ and its SU_3 analogues. Here π-exchange in ρ_{oo} $d\sigma/dt$ is pure spinflip and hence is particularly clean theoretically. We could calculate ρ_{oo} in any frame, but, motivated by the absorption model, let us take it in the s-channel (helicity) frame. First, consider the theoretical background.

The ρ-A_2 Quartet

This spinflip vector meson data is very similar theoretically to the dominantly spinflip ρ-A_2 exchange reactions $\pi^- p \to \pi^o n$, $\pi^- p \to \eta n$, $K^- p \to \bar{K}^o n$ and $K^+ n \to K^o p$. Idealized $d\sigma/dt$ data for the latter processes are indicated in Fig. 5. The dip structure at $-.6$ $(GeV/c)^2$ is well known to be in magnificent agreement with Regge pole theory which predicts.

Reaction	Exchange	
$1/2(\pi^- p \to \pi^o n)$	$\lvert\rho\rvert^2$	(13a)
$3/2(\pi^- p \to \eta^o n)$	$\lvert A_2\rvert^2$	(13b)
$K^- p \to \bar{K}^o n$	$\lvert\rho + A_2\rvert^2$	(13c)
$K^+ n \to K^o p$	$\lvert\rho - A_2\rvert^2$	(13d)

The t-dependence at $-.6$ $(GeV/c)^2$ then follows simply from the ρ and A_2 signature factors--summarized below in terms of the real and imaginary

parts of their amplitudes.

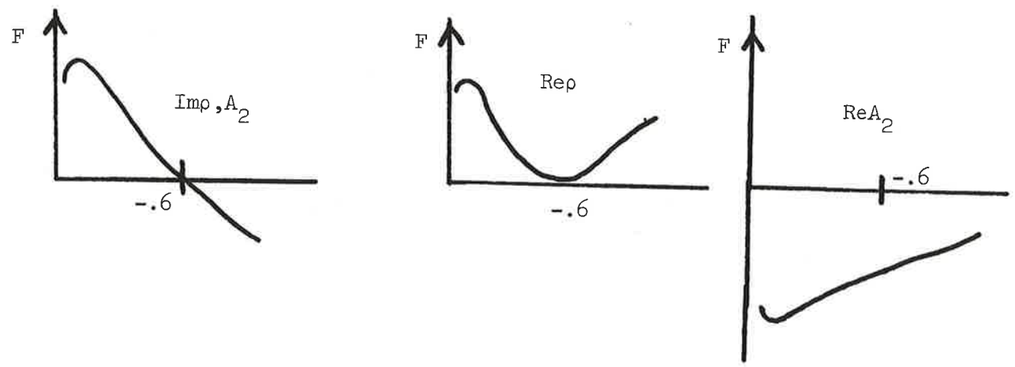

We cannot do justice to all the theoretical effort[2,3,6,7] but just let us note:

(i) The absorption model[3] would predict a dip in all four reactions at $t \simeq -.6$ $(GeV/c)^2$. This contradicts the data (cf. Fig. 5) and this failure is currently understood in terms of absorption correctly giving ImF_{ρ,A_2} but predicting imaginary and real parts of amplitudes to have similar t-dependence: the latter is in disagreement with both data and Regge pole theory.

(ii) To explain the embarrassing success, for our noble quartet, of Regge pole theory--a model which is often a disastrous failure--Chiu[6] has proposed that Regge pole theory is always perfect in spinflip amplitudes.

(iii) Harari[7] suggests that the absorption model is always right for the imaginary parts of amplitudes. In the happy circumstance that the absorption zero coincides with a Regge pole imaginary part zero (as it does for ρ, A_2 exchange in spinflip amplitudes, he predicts that Regge pole theory will describe the real part. In the general case of unhappy amplitudes where this coincidence does not occur, the real parts are unpredictable.

Vector-Meson Quartet

Meanwhile, down on the farm, the π has been quietly munching hay but it perks up as now we return and, by analogy to Eq.(13), consider $\rho_{oo}\, d\sigma/dt$ for:

Reaction	Exchange	
$1/2(\pi^- p \to \rho^o n)$ or $\pi^\pm p \to \rho^\pm p$	$\lvert\pi\rvert^2$	(14a)
$1/2(\pi^+ n \to \omega^o p)$	$\lvert B\rvert^2$	(14b)
$K^- p \to \bar{K}^{o*} n$	$\lvert\pi + B\rvert^2$	(14c)
$K^+ n \to K^{o*} p$	$\lvert\pi - B\rvert^2$	(14d)

where we have normalized so that SU_3 gives

$$2[(14a) + (14b)] = (14c) + (14d)$$

or

$$(14c) = (14d) = (14a) + (14b) \qquad (15)$$

if there is no line-reversal differences between (14c) and (14d). Now, based on previous discussion of the ρ-A_2 exchange data, we consider the predictions of four theories:

(i) Pure absorption[3]: There is a dip in all four reactions at $t \simeq -0.6$ $(GeV/c)^2$.

(ii) Almost any other theory in the SU_6 limit: The trajectories are indicated in Fig. 6 (top) and this makes it clear that, in the sadly unrealistic SU_6 world, the π should behave just like the ρ-exchange and the B just like A_2-exchange. Correspondingly, comparing Eqs.(13) and (14), we see that $\pi^- p \to \rho^o n$ is like $\pi^- p \to \pi^o n$ and should have a dip at $t = -.6$ $(GeV/c)^2$ while the other

three reactions (14b→d) are like $\pi^- p \to \eta n$ and KN CEX, i.e., smooth and nonvanishing there.

(iii) Regge pole theory: realistic trajectories: This is indicated in Fig. 6 (bottom) and is just as (ii) except (14a) should vanish $t \simeq -1.1$ $(GeV/c)^2$ $[\alpha_\pi = -1 \simeq 0.9\,(t - m_\pi^2)]$. At $t \simeq -0.6$ $(GeV/c)^2$, $(14a)/(14b) = \cot^2 \pi\alpha_\pi/2$ from EXD. This is then the model of Chiu[6] with no cut corrections in spinflip amplitudes.

(iv) Hybrid model of Harari[7]: Absorption zeros at -0.6 $(GeV/c)^2$ in imaginary parts. The real parts are unhappy and hence unknown because the absorption dip (−0.6) no longer coincides with the WSNZ ($\alpha_\pi = -1$). Note that in the SU_6 limit, (ii) the amplitudes are happy and the real parts of Regge pole theory are expected to be reliable. In the realistic limit perhaps--mirabile dictu and Sic Transit analyticity--the real parts are still given by EXD Regge pole theory. Then $(14a)/(14b) = \cot^4 \pi\alpha_\pi/2$ at $t \simeq -0.6$ $(GeV/c)^2$. (iv) is distinguished from (iii) because at $t \simeq -1.1$ $(GeV/c)^2$, the imaginary part in (iv) is non-zero and there is no $\alpha_\pi = -1$ dip.

The expectation for the relative values of $\rho_{oo}\, d\sigma/dt$ near $t \simeq -0.6$ $(GeV/c)^2$ is summarized in the table below: here the results for (14c,d) are found from (15).

	$1/2(\pi^+ n \to \omega^o p)$	$1/2(\pi^- p \to \rho^o n)$	$K^- p \to \bar{K}^{*o} n = K^+ n \to K^{*o} p$
Pure absorption	0	0	0
SU_6	1	0	1
Regge	1	1	2
Regge real: Zero Im	1	1	2

The experimental data for ρ_{oo} in the helicity frame is shown in Figs. 7

through 11. I have multiplied the data of Figs. 7 to 10 by $e^{-4t}\ (p_{lab}/5)^2$ to clarify the presentation. The statistics of the higher energy data for $\pi^+ n \to \omega^o p$ shown in Fig. 7 could be usefully improved. However, it seems reasonable to deduce that $\pi^+ n \to \omega^o p$ does not dip near $t \simeq -0.6\ (GeV/c)^2$ and is quite smooth near there. This then agrees with theories (ii) to (iv) and rules out the pure absorption model--theory (i). This is the same disagreement noted in the ρ-A_2 exchange quartet. There the nonvanishing of $\pi^- p \to \eta^o n$ at $t = 0.6\ (GeV/c)^2$ was attributed to the failure of absorption for the real part. In the SU_6 limit exactly, and approximately in the real world, B-exchange is purely real at $t \simeq -.6$ and $\pi^+ n \to \omega^o p$ quite analogous to $\pi^- p \to \eta n$. For reference on this and the following ρ and ω figures, we mark the magic line 0.15 which gives a reasonable representation for $1/2\ e^{-4t}\ (p_{lab}/5)^2\ \rho_{oo}\ d\sigma/dt$ in $\pi^+ n \to \omega^o p$ at the higher energies. In the K^* figures--motivated by the last two theories--we mark double this.

$\overset{(-)}{K}N \to \overset{(-)}{K}{}^*N$ is shown on the next figure (no. 8). It is very striking that the forward peak due to π-exchange is followed by a sharp break which has a similar magnitude and t-dependence to sad old $\pi N \to \omega N$ --which has struggled along with this staid t-dependence right from the forward direction. the $\overset{(-)}{K}{}^*$ data seems again to prefer no dip around -0.6 but it is a brave man who comments on the normalization (given the standard background and resonance definition ambiguities). If anything, theories (iii) and (iv) with $\overset{(-)}{K}{}^* = 2(\omega)$ are favored but decisive tests await new data. The behavior after the break in $\pi N \to \rho N$, shown in Figs. 9 to 11, is again strikingly similar to the ω data. However, the data is inconclusive as to the presence or absence of a dip near $t \simeq -0.6\ (GeV/c)^2$. Thus it is clearly not present below 3 GeV/c

(where background problems are severe), but the beautiful data at 6.95 GeV/c just runs out of statistics at the vital point.

Note the utility of the $\pi N \to \omega N$ "universal" high energy curve $\rho_{oo}\ d\sigma/dt = 0.3\ e^{4t}\ (p_{lab}/5)^{-2}\ mb/(GeV/c)^2$ marked in Figures 7 to 11. This provides a benchmark for distinguishing a dip from a break: it is clear from the theoretical discussion that for $d\sigma/dt$ to have a dip, it should be lower than the "universal" curve. For this reason we consider, for instance, the pretty new $\pi^+ p \to \rho^+ p$ data[27] in Fig. 11 to have a break, not a dip, at $t \simeq -.5\ (GeV/c)^2$.

To summarize, we have shown that the present data (a) have ruled out the pure absorption model[3]--just as did the natural parity exchange quartet; (b) is consistent with the theories (ii) to (iv) above, but theories (iii) and (iv) with no dip in $\pi^- p \to \rho^o n$ are favored by low energy data; (c) further, there are no striking differences in the dip structures for the s and t channels. (See Ref. 2.)

It clearly does not require a great increase in statistics to sharpen these conclusions. These reactions provide very clean tests of theories for the dip structure in a situation (i.e., unhappy amplitudes) which is very different from the well-established natural parity case. The measurements are thus very important.

Finally, we should mention that we have tacitly assumed there is no A_1 (which inhabits n=0 amplitudes) exchange. This can be checked at once by a polarized target experiment[28]. Any non-zero polarization at high energies indicates the presence of the A_1.

C. Large $-t \gtrsim 1$ (GeV/c)^2 and $0 \lesssim b \lesssim .5$ fermi

In this final section I would like to comment on the relevance, for π-exchange processes , of some work, with Charles Chiu, on large -t behavior. As the theory is both rudimentary and speculative, I will be rather brief and let the figures and future data speak for themselves. Further details, especially on the interpretation in the b-plane, may be found in Ref. 2.

Large -t Democracy

In the forward direction, there is a great variety of sizes and shapes for $d\sigma/dt$, e.g., π-exchanges peaks in the sundry Classes I to III, spinflip t=0 dips, absorption -.2, -.6 dips, etc. Figures 2(a) and (b) have already indicated that these differences die away at large -t, where the prodigal ρ has wasted away its π-pole fortune and is reduced to a cross-section similar to that of its poor cousin, the ω. Figure 12 shows this is a universal feature: here we have compiled[29] all $d\sigma/dt$ data at $t = -1$ (GeV/c)^2 and $p_{lab} = 5$ GeV/c . The cross-section universality is particularly striking for the 11 single and double resonance ($\pi^+p \to \rho^+p$ ... $K^-n \to \bar{K}^{*o}\Delta^-$) meson-baryon cross-sections which are all around 30 μb at $t \simeq -1$ (GeV/c)^2 . This effect is illustrated again in Fig. 13 which shows[30] that, whereas at t=0 pp elastic is 50 times bigger than $pp \to N^*_{1688}p$, their ratio is around 1 for $-t \gtrsim 1$ (GeV/c)^2 . Fig. 14 shows a similar effect for photoproduction[8] where the cross-sections are again very different for small -t but have settled down to a monotonous equality by $-t \simeq 1$ (GeV/c)^2 . We deduce that although for small -t there are privileged particles with large cross-sections (e.g., π-poles, elastic scattering), cross sections take on a universal, particle (resonance) independent value at large -t [31]. We term this

Resonance Democracy. The corresponding interpretation in the b-plane is that amplitudes are very particle-dependent for large $b \gtrsim$ o.5 fm , but of some universal size for smaller b. This could even have some relevance for spectroscopy! Thus it becomes as easy to produce interesting particles (e.g., N^*_{1688} in Fig. 13) as it is the standard elder statesmen (e.g., p, Δ, ρ, ...) at large -t: unfortunately perhaps,Fig. 13 shows that democracy produces so many resonances that no single one stands out from the background!

t-Dependence

After considering the size we now turn to t-dependence for $-t \gtrsim 1$ (GeV/c)^2. In photoproduction, there is the reasonably well-established energy independent behavior e^{3t} in this t-region. This was indicated in Fig. 14 but is better demonstrated in Fig. 15 which shows the three processes $\gamma p \to \pi^+ n$, $\gamma p \to \pi^o p$, and $\gamma p \to \pi^- \Delta^{++}$, that have measured[32] up to $-t = 3$ (GeV/c)^2. The situation for strong interactions is much less clear, as there are no measurements in this t-range, $1 \lesssim -t \lesssim 3$ (GeV/c)^2 , above $p_{lab} \gtrsim 5$ GeV/c. Fig. 16 shows one photoproduction and three strong interaction half-asleep π-exchange processes. After normalizing them to the forward π-peak there is a striking similarity in the size and shape of $d\sigma/dt$ for $-t \gtrsim 0.6$ (GeV/c)^2 . This agrees, qualitatively, with vector dominance, and is the best evidence that similar dynamics govern large -t data in both strong interactions and photoproduction. However, the formulation of a universal law is confused by the non-π-exchange data. In fact, both $\pi^+p \to K^+\Sigma^+$ (not shown here--see Ref. 2) and $\pi^-p \to \pi^o n$ fall like $e^{\simeq 3t}$ at $p_{lab} = 5$ GeV/c . $\pi^-p \to \pi^o n$ is shown in Fig. 17, where it is compared with the similar $\gamma p \to \pi^o p$ data, already shown in Fig. 15. Although both reactions, in Fig. 17, fall like e^{3t}, the

coefficient has a different energy dependence in the two cases; photoproduction in the $p_{lab}^2\, d\sigma/dt$ plot is energy independent; $\pi^- p \to \pi^o n$ at $t \simeq -1$ falls by at least a factor of 2 between 5 and 18 GeV/c. Further the dip at $t \simeq -1.4$ $(GeV/c)^2$ in $\pi^- p \to \eta^o n$ and $\pi^+ p \to \eta^o \Delta^{++}$ shown in Figs. 18 and 19 is in clear conflict with the universal e^{3t} behavior deduced from Figures 15 and 16.

Energy Dependence

The e^{3t} photoproduction t-dependence is correlated with a p_{lab}^{-2} behavior. This is summarized in Fig. 20 for the three processes whose t-dependence was discussed in Fig. 15. We use the conventional α_{eff} defined by:

$$d\sigma/dt = A(t)\ (p_{lab})^{2\alpha_{eff}(t)-2} \quad \text{at fixed } t \quad . \tag{16}$$

Fig. 20 is in dramatic contrast to the strong interaction non-π-exchange data in Fig. 21 whose α_{eff} is in striking agreement[35→38] with Regge theory's[39] $\alpha_{eff}(t) \simeq .5 + t$ rather than the, t-independent, $\alpha_{eff}(t) \simeq 0$ of photoproduction. The ηN t-dependence of Figs. 18 and 19 was also an amazing success for Regge theory as the dip position agreed well[33] with the A_2 WSNZ at $\alpha_{A_2} = -1$.

However, we must point out an important experiment bias between strong interaction and photoproduction data: thus both the α_{eff} and ηN dip of Figs. 18, 19, and 21 are determined from data with $p_{lab} \leq 5$ GeV/c: the $p_{lab}^{-2}\ e^{3t}$ behavior of photoproduction in Figs. 14, 15, and 20 is established for $5 \lesssim E_{lab} \lesssim 18$ GeV. In fact, this latter universal behavior is not exhibited by photoproduction for $E_{lab} \lesssim 5$ GeV . This is shown in Fig. 17 for $\gamma p \to \pi^o p$ which also shows marked shrinkage in $E_{lab} \simeq 5$ GeV; further, Figs. 7-11 make it evident that hadronic π-exchange data shrinks for $-t \gtrsim 0.6$ $(GeV/c)^2$ and $p_{lab} \lesssim 5$ GeV/c .

Theoretical Summary

The current large -t data can be summarized by writing for a typical amplitude A

$$A = A_R(s,t) + A_{FP}(s,t) \quad . \tag{17}$$

A_R (R for Regge) has Regge-type s energy dependence and its t-dependence exhibits WSNZ and absorption dips. It perhaps corresponds to high partial $b \gtrsim 0.5$ fm .

A_{FP} (FP for Fixed Pole) is energy-independent ($\alpha_{eff} \simeq 0$) and has an approximately $e^{1.5t}$ t-dependence. Its Fourier-Bessel transform is thus e^{-4b^2} which is dominantly $b \lesssim 0.5$ fm .

Current photoproduction data and strong interaction π-exchange data seem to have a large ratio A_{FP}/A_R so that the A_{FP} dominates for $-t > 1$ $(GeV/c)^2$ and $p_{lab} \gtrsim 5$ GeV/c . For ρ, A_2 and K^*-K^{**} exchange hadronic data, (plus P',ω in elastic scattering) this ratio is much smaller and consistent with zero. If any A_{FP} exists in these reactions it will eventually dominate for $-t > 1$ $(GeV/c)^2$ at high enough incident energies.

It is clear that the experimental bias, i.e., there is no exchange data for hadronic reactions at large -t and $p_{lab} \gtrsim 5$ GeV/c , must be remedied before we ever know the truth.

Numerology

Finally we remind the reader of the striking coincidence between the energy-independent e^{3t} behavior of the two-body processes discussed earlier and the $e^{\simeq -3p_\perp^2}$ behavior observed[40] in inclusive reactions for $p_\perp^2 \gtrsim 0.2$ $(GeV/c)^2$. [Remember t is essentially $-p_\perp^2$ for $2 \to 2$ processes.] The latter is shown

in Fig. 22 at 12 GeV/c [41] and is also energy independent--a similar $p_\perp^2$ dependence is seen at the ISR[42].

We do not dwell on this, for similar techniques relate e^{8t} of diffraction scattering to the eight-fold way. e^{3t} itself is connected not only to the number of quarks in the proton, and the Holy Trinity, but also to Raquel Welch, and whoever may be your favourite figure.

REFERENCES AND FOOTNOTES

1. A. Bialas and K. Zalewski, Nucl. Phys. B6, 449, 465, 478, 483 (1968).
2. G.C. Fox in Phenomenology in Particle Physics 1971, edited by C.B. Chiu, G.C. Fox, and A.J.G. Hey , (Caltech, 1971).
3. M. Ross, F.S. Henyey, and G.L. Kane, Nucl. Phys. 23B, 269 (1970).
4. E.L. Miller, et al., Phys. Rev. Letters 26, 984 (1971).
5. G. Manning, et al., Nuovo Cimento 41A, 167 (1966).
6. C.B. Chiu, Nucl. Phys. B30, 477 (1971), and in UCRL-20655, Proceedings of the Workshop on Particle Physics at Intermediate Energies, edited by R.D. Field.
7. H. Harari, Phys. Rev. Letters 26, 1400 (1971).
8. R. Diebold, SLAC-PUB-673, published in Proceedings of the 1969 Boulder Conference on High Energy Physics, edited by K. Mahanthappa, W. Walker, and W. Brittin,(Colorado Associated University Press, 1970).
9. A.S. Goldhaber, G.C. Fox and C. Quigg, Phys. Letters B30, 249 (1969).
10. G.S. Abrams and U. Maor, Phys. Rev. Letters 25, 621 (1970).
11. Absorption only affects values of $b \leq 1$ fm . It thus is very important in regions B and C but it cannot affect $A_\pi^{HIGH}(t)$.
12. Proceedings of the Conference on $\pi\pi$ and $K\pi$ Interactions, edited by F. Loeffler and E. Malamud (preprint, 1969).
13. G.C. Fox, in High Energy Collisions, edited by C.N. Yang, et al., (Gordon and Breach, Inc., New York 1969).
14. E. Leader, Phys. Rev. 166, 1599 (1968).
15. The PMA model is silent on the question of M=2. Applying PMA to the full

amplitude gives M=2 as described in text. However, an attractive alternative is to apply it to the black box of the quark model. This would be in equally good agreement with current data; but only generate M=0 and 1 (and the relative j-plane simplicity of the 3-pole interpretation in the text).

16. C.F. Cho and J.J. Sakurai, Phys. Rev. D2, 517 (1970).

17. J.D. Jackson and C. Quigg, Phys. Letters 29B, 236 (1968) and Nucl. Phys. B22, 301 (1970).

18. N. Byers, Phys. Rev. 156, 1703 (1967) for crippled π; P.R. Stevens, Phys. Rev. D1, 2523 (1970) for fully-fledged and half-asleep π.

19. D.W.G.S. Leith in Phenomenology in Particle Physics 1971, edited by C.B. Chiu, G.C. Fox, and A.J.G. Hey, (Caltech, 1971).

20. P.K. Williams, Phys. Rev. D1, 1312 (1970). The attribution of (equal) form factors in this reference to flip and nonflip amplitudes is both dubious and outside the spirit of PMA. To the extent such things matter, PMA cannot be trusted.

21. Equation (10) holds at $t=0$. ρ^H_{oo} has extra t-dependence $1/(t-m_\pi^2)^2$ but $2\rho^H_{11}$ is proportional to $\left[1 + (t/m_\pi^2)^2\right]/(t-m_\pi^2)^2$. (The $(t/m_\pi^2)^2$ term comes from the s-channel double flip amplitude.)

22. The PMA model allows an estimate of the contribution of the "different amplitudes", e.g., $2\rho^H_{11}\, d\sigma/dt$ for $\pi^- p \to \rho^o n$, that are nonvanishing at t=0 and obscure the genuine half-asleep π contribution. See C.D. Froggatt and D. Morgan, Phys. Rev. 187, 2044 (1969).

23. $\bar{p}\Delta^{++}$ helicity nonflip is half-asleep, the helicity flip one vertices make up the crippled π component.

24. The same interference between π and ρ exchange--again with a sign in agreement with the quark model--can be used to explain the difference between $K^+n \to K^{*o}p$ and $K^-p \to \bar{K}^{*o}n$. See G.C. Fox, et al., "The Charge Exchange Production Mechanism for the $K^*(890)$", Argonne preprint, (1971).

25. G.S. Abrams, et al., Phys. Rev. Letters 25, 617 (1970).

26. I.J. Bloodworth, et al., "$\Delta^{++}\rho^o$ and $\Delta^{++}\omega^o$ Final States at 5.45 GeV/c", Toronto preprint (1971).

27. W. Michael, G. Gidal, and D. Grether, "The Reaction $\pi^+p \to \rho^+p$ at 2.67 GeV/c", LBL preprint (1971).

28. G.C. Fox, "Past Lessons and Future Dreams from Polarization Data in High Energy Physics", invited talk at the Berkeley Polarization Conference, August, 1971.

29. The plotted points are determined by interpolation of data at energies around 5 GeV/c. Details and explicit references may be presented elsewhere.

30. U. Amaldi, et al., Phys. Letters 34B, 435 (1971).

31. This is decidedly glib. Thus Fig. 12 shows there is still some (albeit not as much as at t=0) correlation of the size of $d\sigma/dt$ at $t = -1$ $(GeV/c)^2$ with t-channel quantum numbers. For instance, Fig. 12 shows the natural ordering: Pomeron > meson S=0 > meson S=1 > baryon S=0 > baryon S=1 exchange. In more detail, we find $\tau P+ > \tau P-$ meson exchange, proton induced > similar meson-induced reactions (as expected in the quark model). In Fig. 12 the photoproduction data has been scaled by the natural coefficient 550, (for $\gamma_\rho^2/4\pi = 0.5$) so that VDM predicts,for

instance, (scaled) $\gamma p \to \pi^+ n = 2\rho_{11}^H \, d\sigma/dt \, (\pi^- p \to \rho^o n)$. It is noteworthy that--in disagreement with exact VDM--photoproduction is larger than strong interaction data. This was also indicated in Fig. 3.

32. P. Joos, DESY-HERA 70-1, and $\gamma p \to \pi^o p$ large -t data from Caltech Users Group (private communication).

33. The EXD prediction $d\sigma/dt \, (\pi^- p \to \eta^o n) = 2/3 \cos^2 (\pi\alpha/2) \, d\sigma/dt \, (K^- p \to \bar{K}^o n)$ is shown in Fig. 18(c), for $\alpha = \alpha_{A_2} = 0.4 + .9t$.

34. E.H. Harvey, et al., "The Reaction $\pi^- p \to \gamma\gamma n$ at 3.65 GeV/c", preprint, 1971.

35. R.A. Sidwell, et al., Phys. Rev. D3, 1523 (1971).

36. V. Barger and R.J.N. Phillips, "Deductions from New $\pi^- p \to \pi^o n$ Data at Large Momentum Transfers", preprint, 1971.

37. B.B. Brabson, et al., Phys. Rev. Letters 25, 553 (1970).

38. C. Schmid in Phenomenology in Particle Physics 1971, edited by C.B. Chiu, G.C. Fox, and A.J.G. Hey, (Caltech, 1971).

39. For a theoretical interpretation of this shrinkage in terms of dual models, see A. Krzywicki,"Large Angle Scattering of Hadrons" in High Energy Phenomenology, edited by J. Tran Thanh Van (Saclay, 1971)

40. E.L. Berger (particularly pages 176-179) in Phenomenology in Particle Physics 1971, edited by C.B. Chiu, G.C. Fox, and A.J.G. Hey (Caltech, 1971).

41. C.W. Akerlof, et al., Phys. Rev. D3, 645 (1971).

42. Argonne-Bologna-Michigan Collaboration: reliable rumor that ISR inclusive data is $e^{\simeq -3.5 p_\perp^2}$ for $p_I^2 \gtrsim .2 \text{ (GeV/c)}^2$.

44. J.A.J. Matthews, et al., Phys. Rev. Letters 26, 400 (1971) and "Regge Analyses of ρ^o Production in πN Charge Exchange Channels at 7 GeV/c", Toronto preprint, 1971.

43. J.A. Gaidos, et al., Phys. Rev. D1, 3190 (1970). (13.1 GeV/c); N.N. Biswas, et al., preprint (1970) (18.5 GeV/c); ABC Collaboration, Nucl. Phys. B8, 45 (1968) (8 GeV/c).

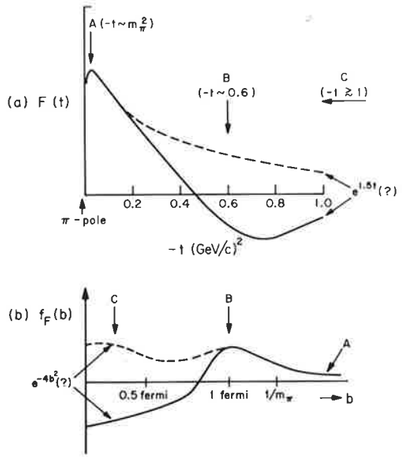

Fig. 1

The three distinct regions for π-exchange amplitudes studied in this paper. They are marked both in the momentum transfer t-plane and in their roughly corresponding positions in the impact parameter b-plane.

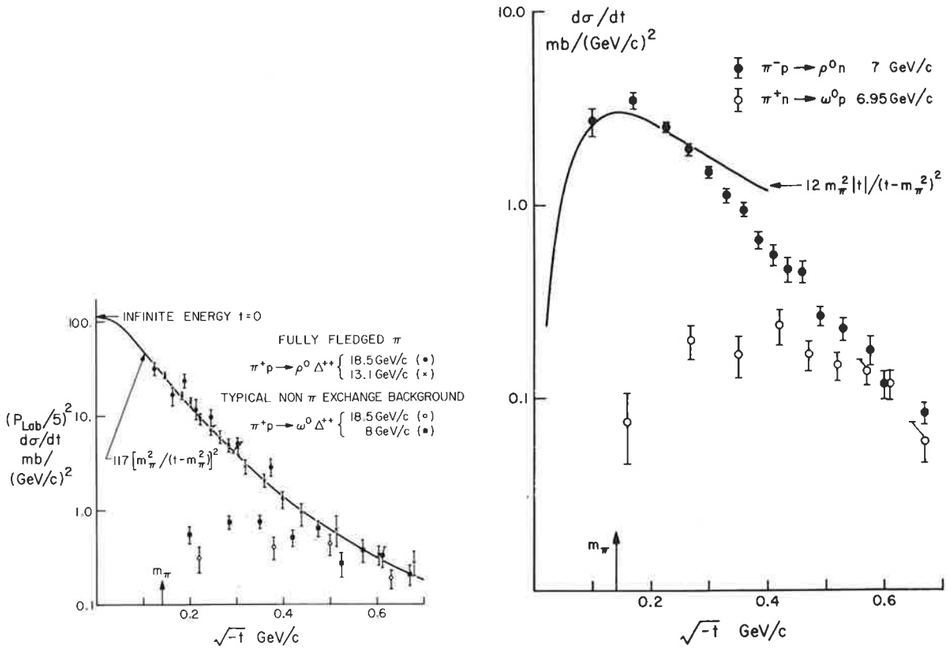

Fig. 2. (a) FULLY-FLEDGED π: a comparison of $\pi^+p \to \rho^0\Delta^{++}$ and $\pi^+p \to \omega^0\Delta^{++}$ for small -t (data from Ref. 43). (b) HALF-ASLEEP π: a comparison of $\pi^-p \to \rho^0 n$ and $\pi^+n \to \omega^0 p$ for small -t (data from Ref. 44). The solid curves are eyeball fits. The greater vitality and hence usefulness for studying π-π scattering of the fully-fledged π is apparent.

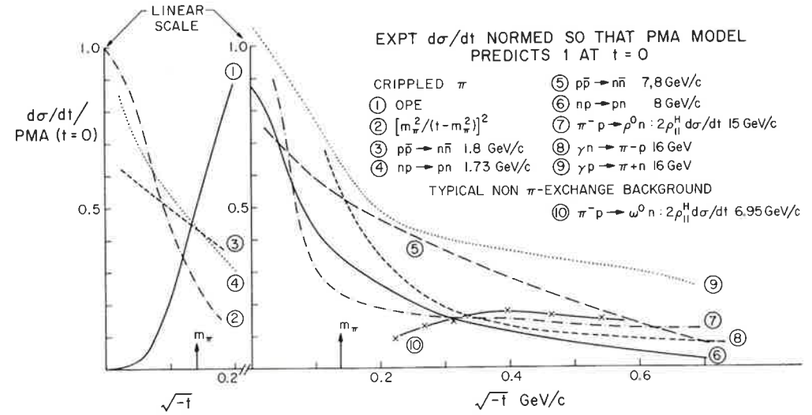

Fig. 3. Crippled π dσ/dt normalized so that Poor Man's Absorption predicts 1 at t = 0. OPE represents $2[t/(m_\pi^2 - t)]^2$ and the data sources are cited in Ref. 2.

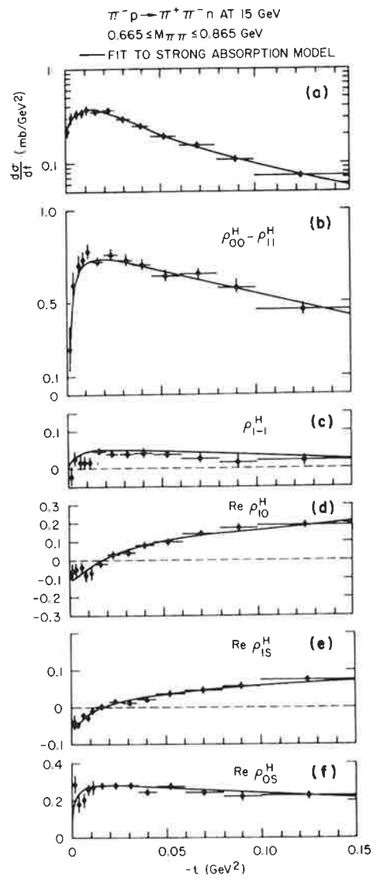

Fig. 4

The differential cross-section and density matrix elements in the helicity frame for $\pi^-p \to \pi^+\pi^-n$ at 15 GeV/c. The data are from Ref. 19 and the curves represented a fit to the Poor Man's Absorption model: the predictions of which, in $\pi N \to \rho N$ come from Williams (Ref. 20).

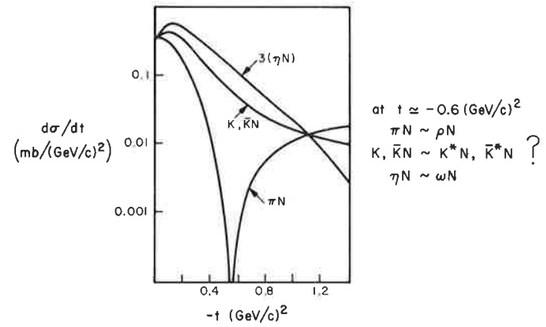

Fig. 5. An indication from Ref. 6 of the t-dependence of the spinflip parts of the four simple ρ,A_2 exchange reactions, i.e., $\pi^- p \to \pi^0 n$ (ρ only), $\pi^- p \to \eta n$ (A_2 only), $K^- p \to \bar{K}^0 n$, $K^+ n \to K^0 p$ ($\rho \pm A_2$). As indicated on the figure, one might expect a similar behavior at $t \simeq -0.6\ (\mathrm{GeV}/c)^2$ for $\rho_{00}\ d\sigma/dt$ in the four spinflip vector meson production reactions ($\pi^- p \to \rho^0 n$, $\pi^- p \to \omega^0 n$, $K^- p \to \bar{K}^{*0} n$, $K^+ n \to K^{*0} p$).

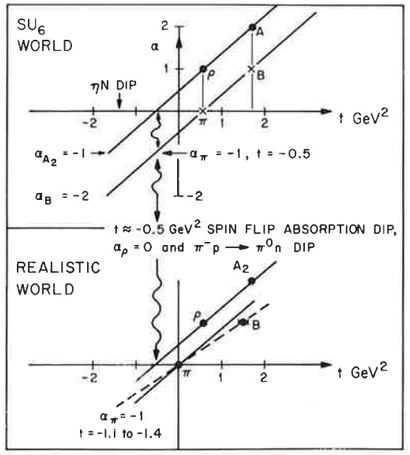

Fig. 6

The plot of π, B, ρ, and A_2 trajectories and their associated WSNZ t-values in (a) the SU_6 and (b) the sadly distorted realistic world. In (b) we mark two possible π trajectories, one with canonical slope parallel to the ρ-A_2 trajectory and one with a lower slope passing through its EXD partner--the B meson. It is curious that the mass of the B is half-way between its SU_6 value and that predicted from $l = -0.02 + 0.9\ m_B^2$ (a normal slope trajectory through the real live π).

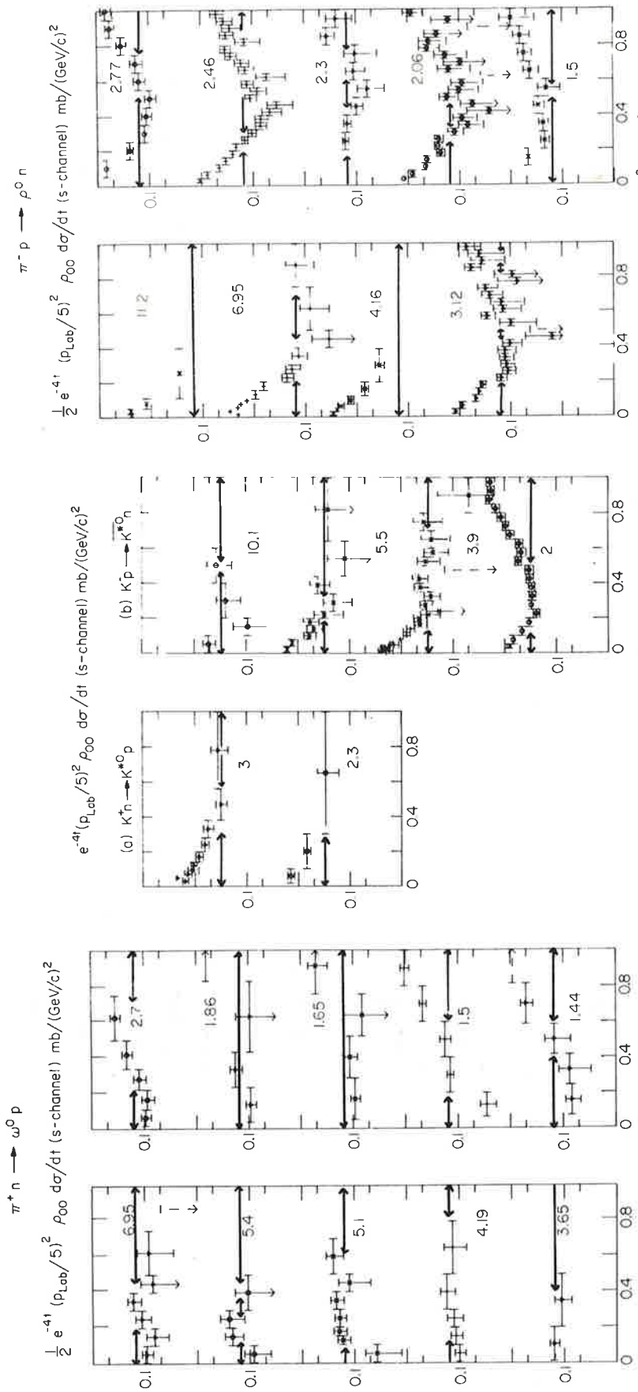

Fig. 8

s-channel $\rho_{00}\ d\sigma/dt$ for (a) $K^+ n \to K^{*0} p$, (b) $K^- p \to \bar{K}^{*0} n$ (data sources are cited in Ref. 2). Solid line marks 0.15: approximate "fit" to $\pi N \to \omega N$.

Fig. 7

s-channel $\rho_{00}\ d\sigma/dt$ for $\pi^+ n \to \omega^0 p$ (data sources are cited in Ref. 2). Solid line marks 0.15: approximate "fit" to $\pi N \to \omega N$ at high energy.

Fig. 9

s-channel $\rho_{00}\ d\sigma/dt$ for $\pi^- p \to \rho^0 n$ and $\pi^+ n \to \rho^0 p$ (data sources are cited in Ref. 2). Solid line marks 0.15: approximate "fit" to $\pi N \to \omega N$.

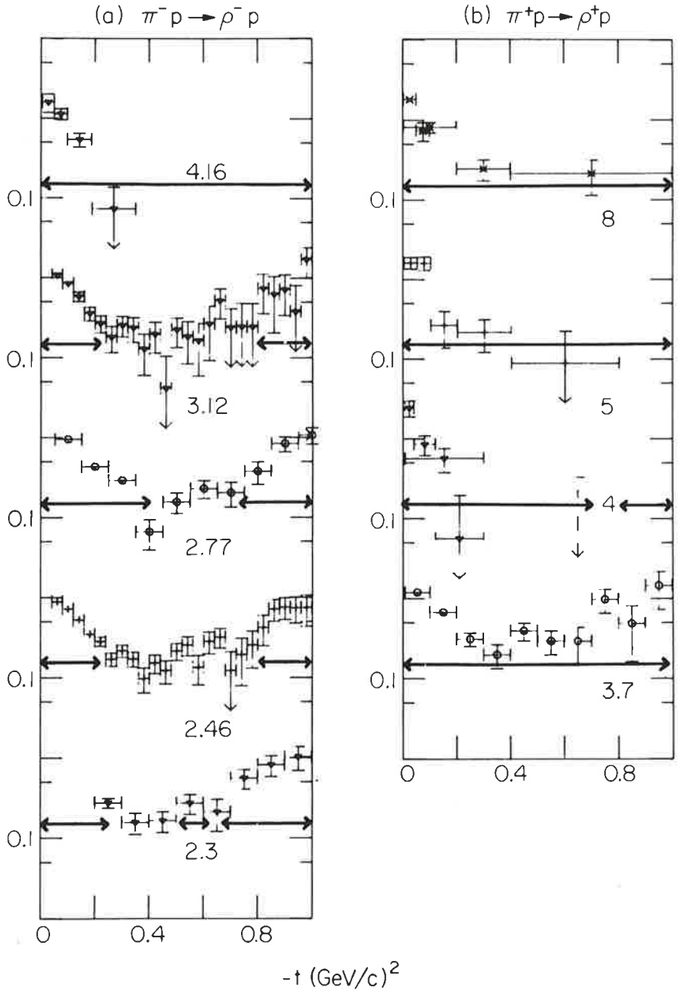

Fig. 10. s-channel $\rho_{00}\ d\sigma/dt$ for (a) $\pi^- p \to \rho^- p$ and (b) $\pi^+ p \to \rho^+ p$ (data sources are cited in Ref. 2). Solid line marks 0.15: approximate "fit" to $\pi N \to \omega N$.

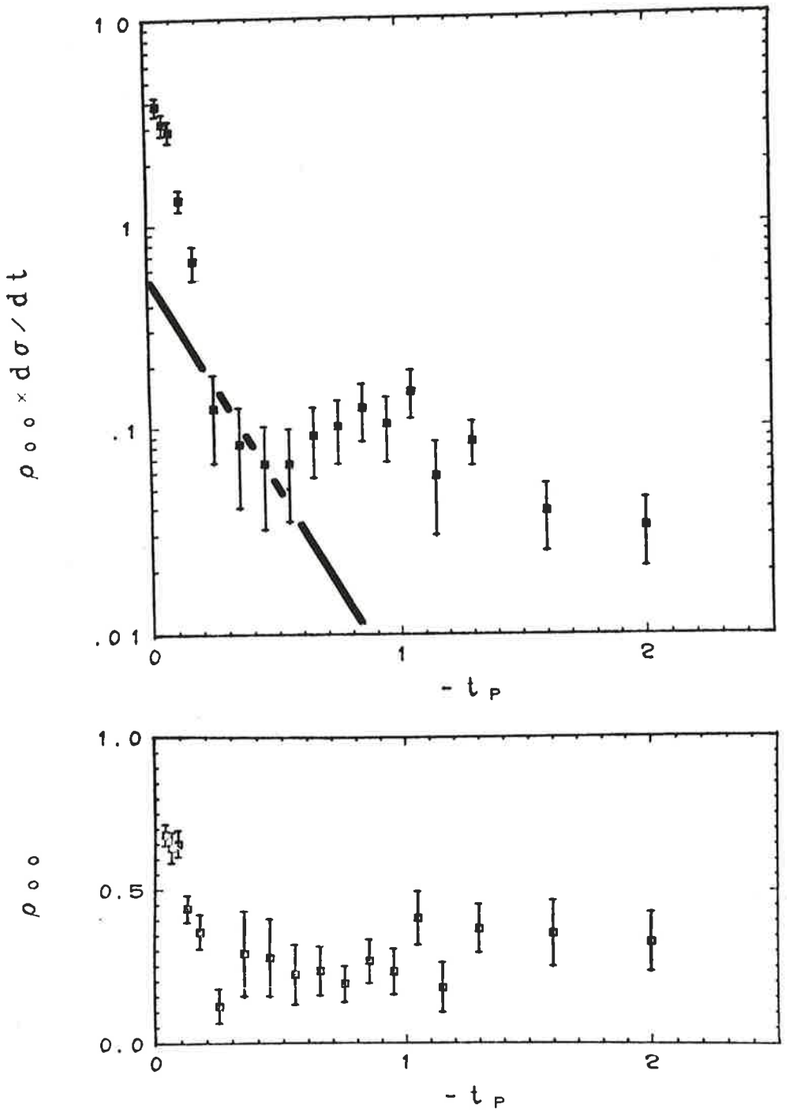

Fig. 11. Recent data on $\rho_{00}\ d\sigma/dt$ (helicity frame) in $\pi^+ p \to \rho^+ p$ (Ref. 27). The solid curve is the "universal" ωN curve 0.15 $(p_{lab}/5)^{-2}\ e^{4t}$ also marked on Figs. 7-10. This crosses the data at $t \simeq -0.6$ $(GeV/c)^2$ in agreement with the previous figures. This disagreement between data and universal curve at large -t is attributed to the low beam momentum. [Cf. $\pi N \to \omega N$ $p_{lab} \lesssim 2.7$ GeV/c, Fig. 7; $K^- p \to \bar{K}^{*0} n$, 2 GeV/c, Fig. 8; and similar low-energy ρN data in Figs. 9 and 10.]

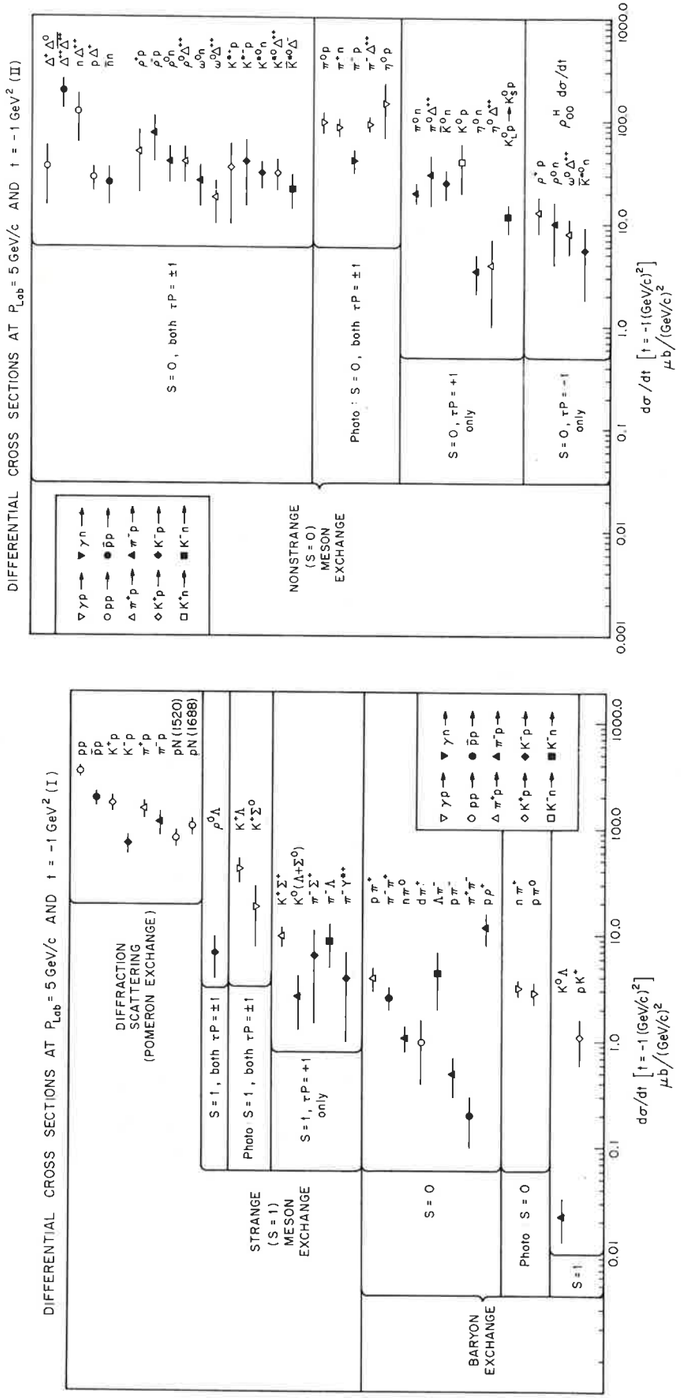

Fig. 12. Resonance democracy at large -t: A compilation in two parts of $d\sigma/dt$ at $t \simeq -1$ (GeV/c)^2 and P_{lab} = 5 GeV/c. Photoproduction has been scaled by the 550 suggested by VDM and $\gamma_\rho^2/4\pi$ = 0.5. This reports unpublished work with Charles Chiu.

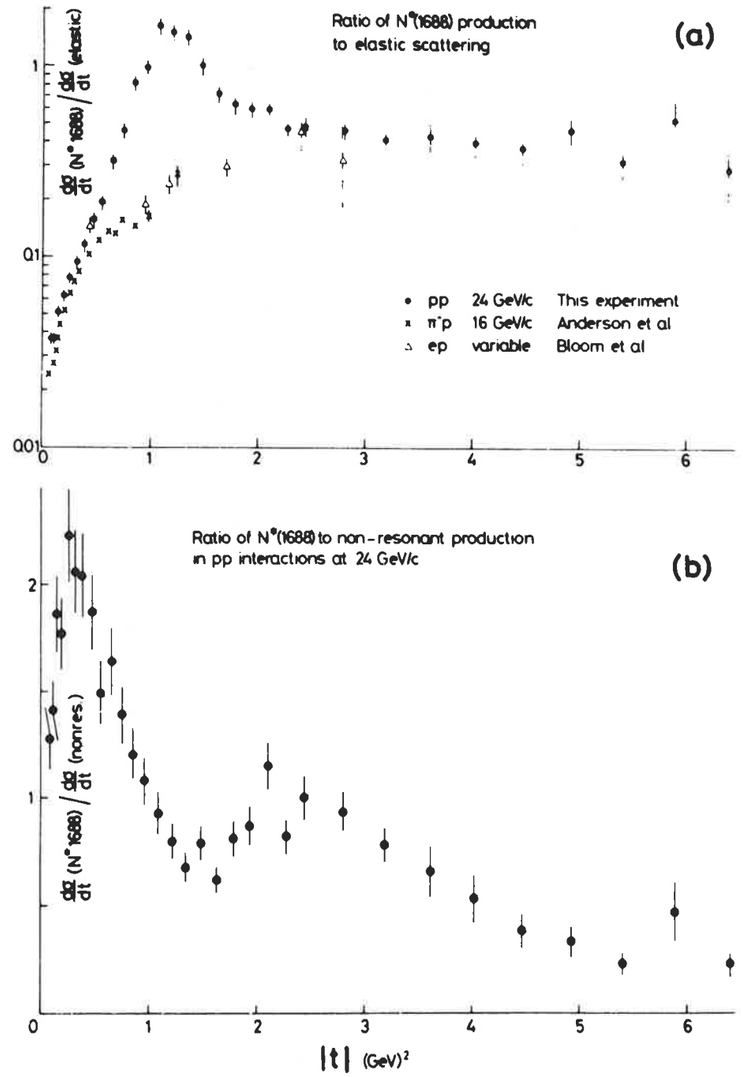

Fig. 13. Resonance democracy at large -t: (Ref. 30) (a) The ratio of N^*_{1688} production to elastic scattering in 24 GeV/c pp, 16 GeV/c π^-p, and high energy ep reactions, as a function of t. (b) Ratio of N^*_{1688} to non-resonant continuum (defined as 1.61 ≤ missing mass ≤ 1.78 GeV) production in 24 GeV/c pp reactions. Interpreting "non-resonant" as a sum of low-spin high-width resonances, both figures indicate that whereas at small -t there is a wide range of cross-sections (p >> N^*_{1688} > non-resonant), at large -t all particles/resonances are produced with roughly the same cross-section.

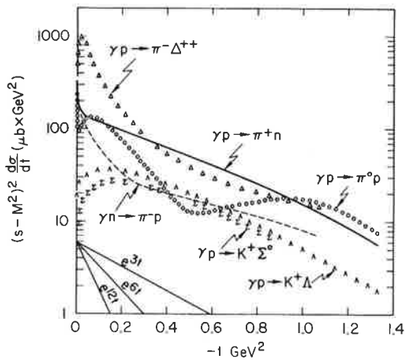

Fig. 14

Schematic representation of the universal $(s - m^2)^2\, d\sigma/dt$ curves for photoproduction (Ref. 8).

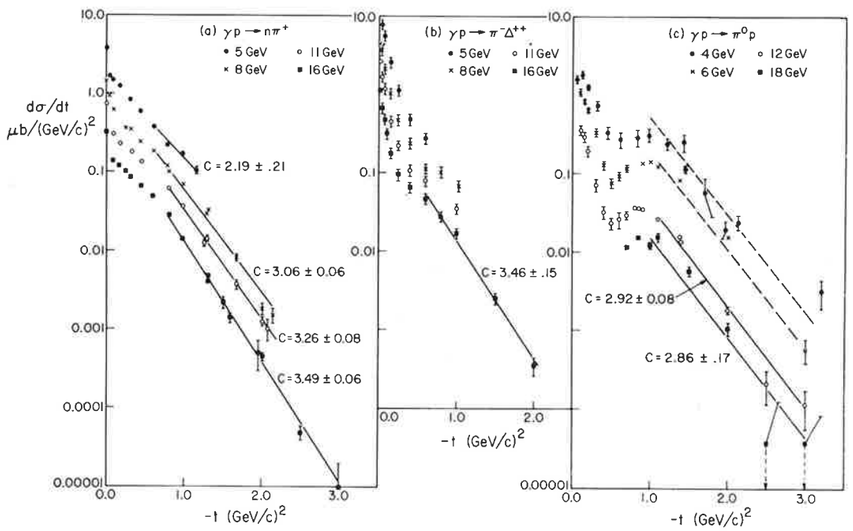

Fig. 15. A compilation of large -t data in photoproduction (a) $\gamma p \to \pi^+ n$, (b) $\gamma p \to \pi^- \Delta^{++}$, and (c) $\gamma p \to \pi^0 p$, from reference 32. Marked are $\exp(c \pm \Delta c)$ fits for $-t > 0.5$ (a, b) and $-t > 1$ (GeV/c)^2 (c). The dashed lines in (c) correspond to 12 GeV fitted slope $c = 2.92$. (The fitted exponential at 6 GeV is a very poor fit, cf. Fig. 17: that at 4 GeV is poorly determined.) This figure is only intended to indicate the approximately universal t-dependence: the behavior with energy is better summarized in Fig. 20.

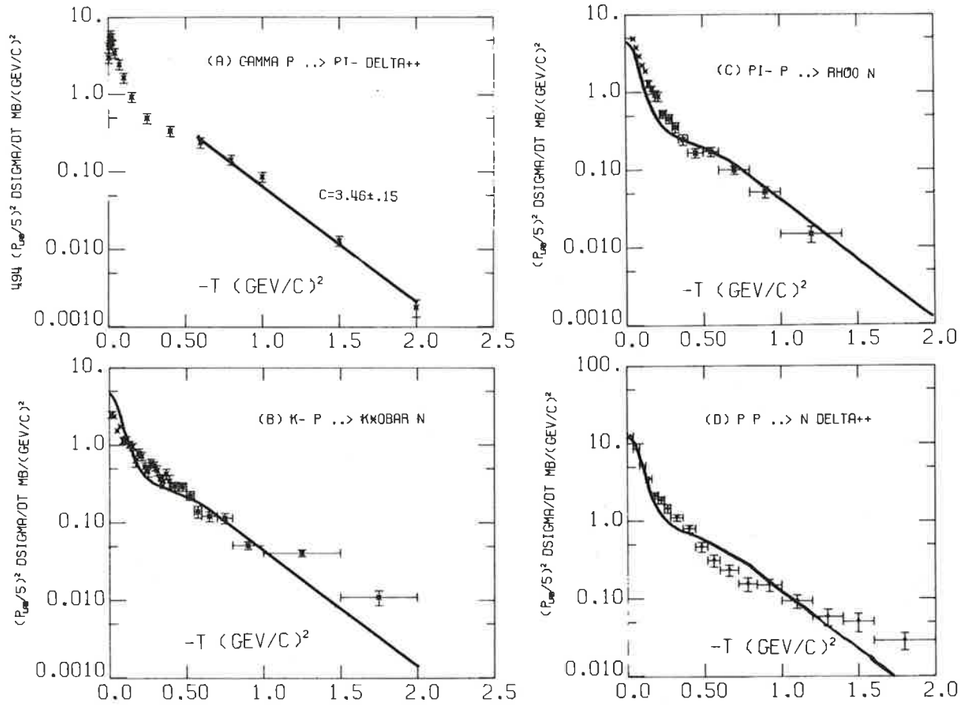

Fig. 16. Half-asleep π-exchange reactions: $(p_{lab}/5)^2\, d\sigma/dt$ for: (a) 494 $(\gamma p \to \pi^- \Delta^{++})$ at 16 GeV; (b) $K^- p \to \bar{K}^{*0} n$ at 3.9 GeV/c; (c) $\pi^- p \to \rho^0 n$ at 6.95 GeV/c; and (d) $pp \to n\Delta^{++}$ at 6.6 GeV/c. Exponential fit in (a) is that shown in Fig. 15. Solid curves on (b) through (d) are the 16 GeV $\gamma p \to \pi^- \Delta^{++}$ in (a) scaled to reproduce the trend of the strong interaction data. These curves show that for reactions going by π-exchange there is little qualitative difference between photoproduction and strong interactions.

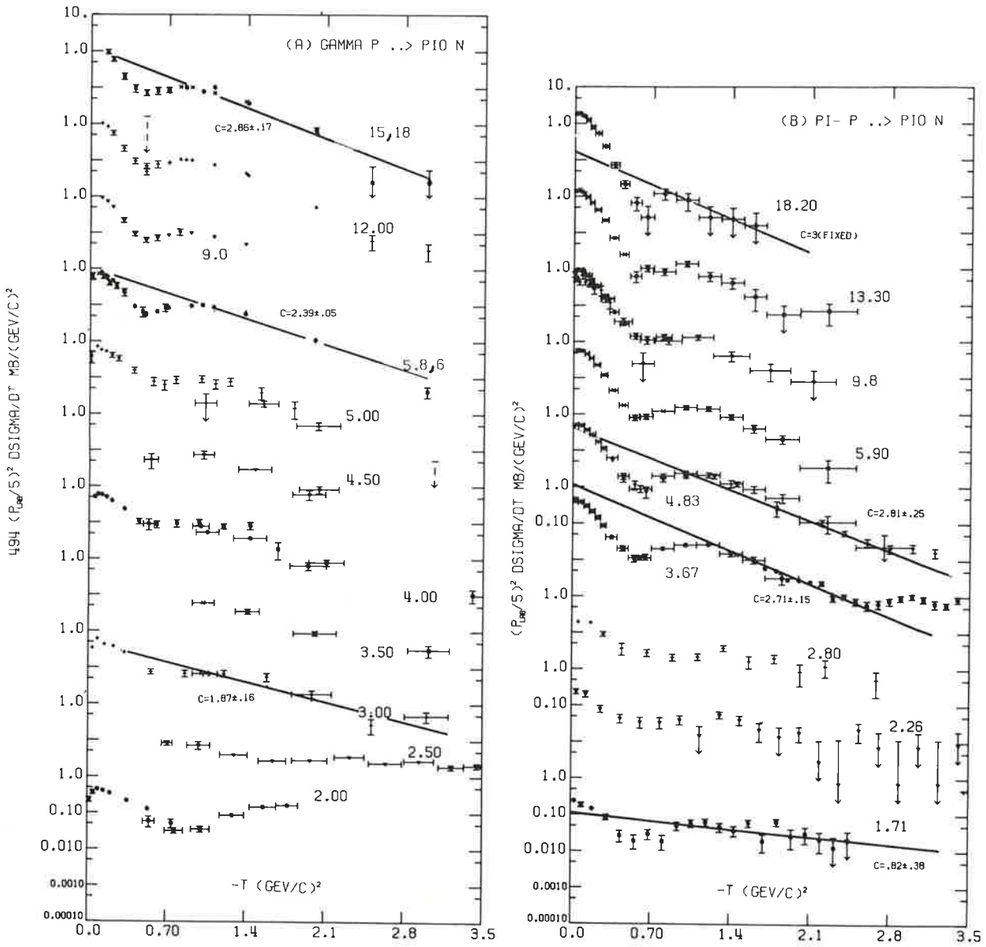

Fig. 17. Forward dip reactions (a) 494 $(E_{lab}/5)^2$ $d\sigma/dt$ mb/$(GeV/c)^2$ for $\gamma p \to \pi^\circ p$. Coefficient 494 is suggested by VDM for $\gamma_\rho^2/4\pi = 0.45$. (b) $(p_{lab}/5)^2$ $d\sigma/dt$ mb/$(GeV/c)^2$ for $\pi^- p \to \pi^\circ n$. A selection of exponential fits $e^{[c\pm\Delta c]t}$ to the large -t data are also shown. Note particularly the energy variation of the t = 0 intercepts of both the large -t fits and $d\sigma/dt$ itself. These give the sizes of A_{FP} and A_R in Eq. (17).

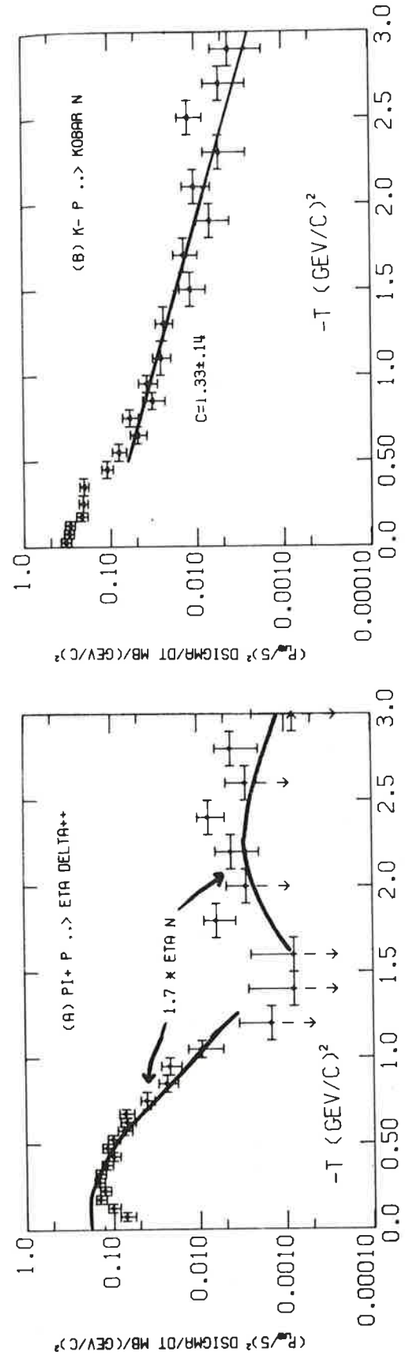

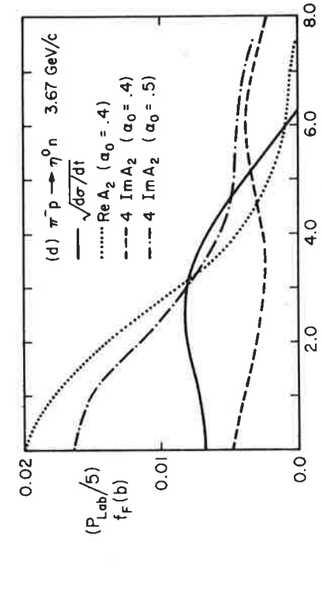

Fig. 18. Patchwork quilt of Regge in Wonderland up to t = -3 $(GeV/c)^2$. $(p_{lab}/5)^2$ $d\sigma/dt$ for (a) $\pi^+ p \to \eta^\circ \Delta^{++}$ at 3.5 GeV/c, (b) $K^- p \to \bar{K}^\circ n$ at 3.95 GeV/c, (c) $\pi^- p \to \eta^\circ n$ at 3.72 (x), 3.67 (▲), and 4.83 (●) GeV/c. The data sources are cited in Ref. 2. In (b) we show an exponential fit to the large -t data. The attribution of the dip in (a) and (c) to the $\alpha A_2 = -1$ WSNZ is confirmed by the solid line in (a) which is 1.7 x the ηn data at 3.67, 3.72 in (c). The deviation near t = 0 is due to nonflip component of ηn $(\eta\Delta^{++}$ is purely flip). Further solid curve in (c) is Regge pole prediction (Ref. 33) based on EXD and data in (b). The empirical partial wave analysis shown in (d) is described in Ref. 2.

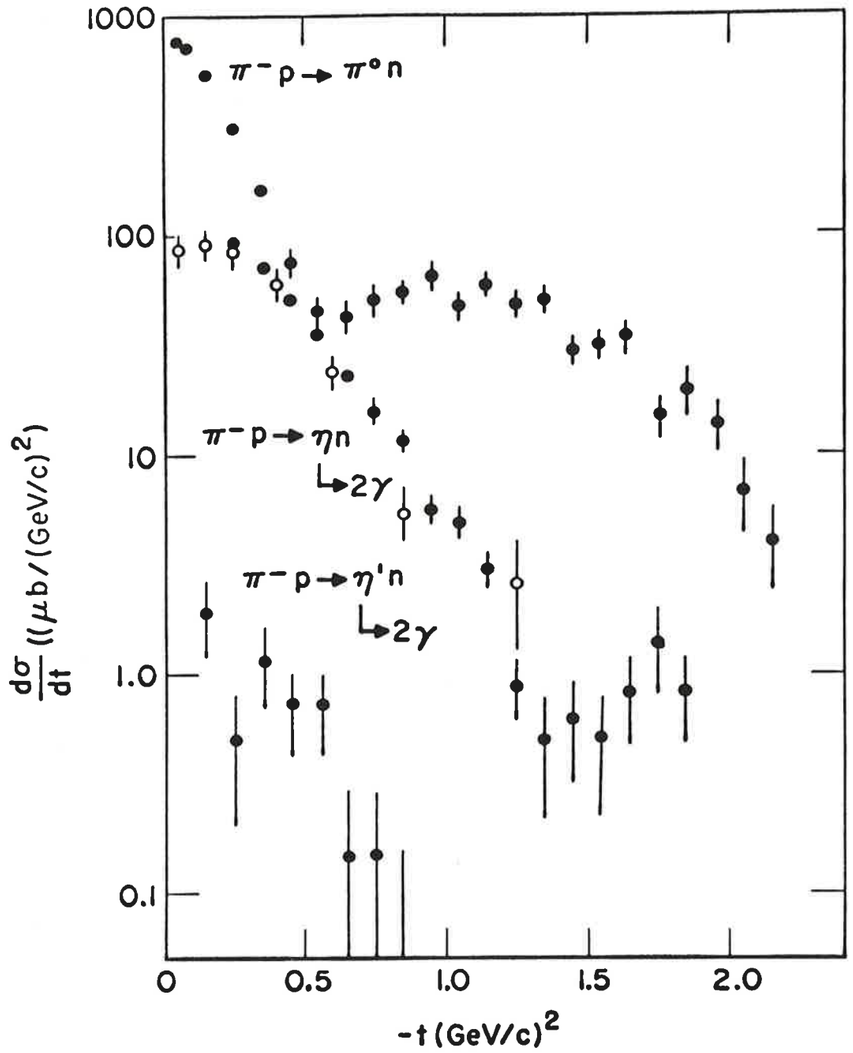

Fig. 19. New data from Ref. 34 at 3.65 GeV/c confirming the dip at $t \simeq -1.4$ (GeV/c)^2 in $\pi^- p \to \eta n$.

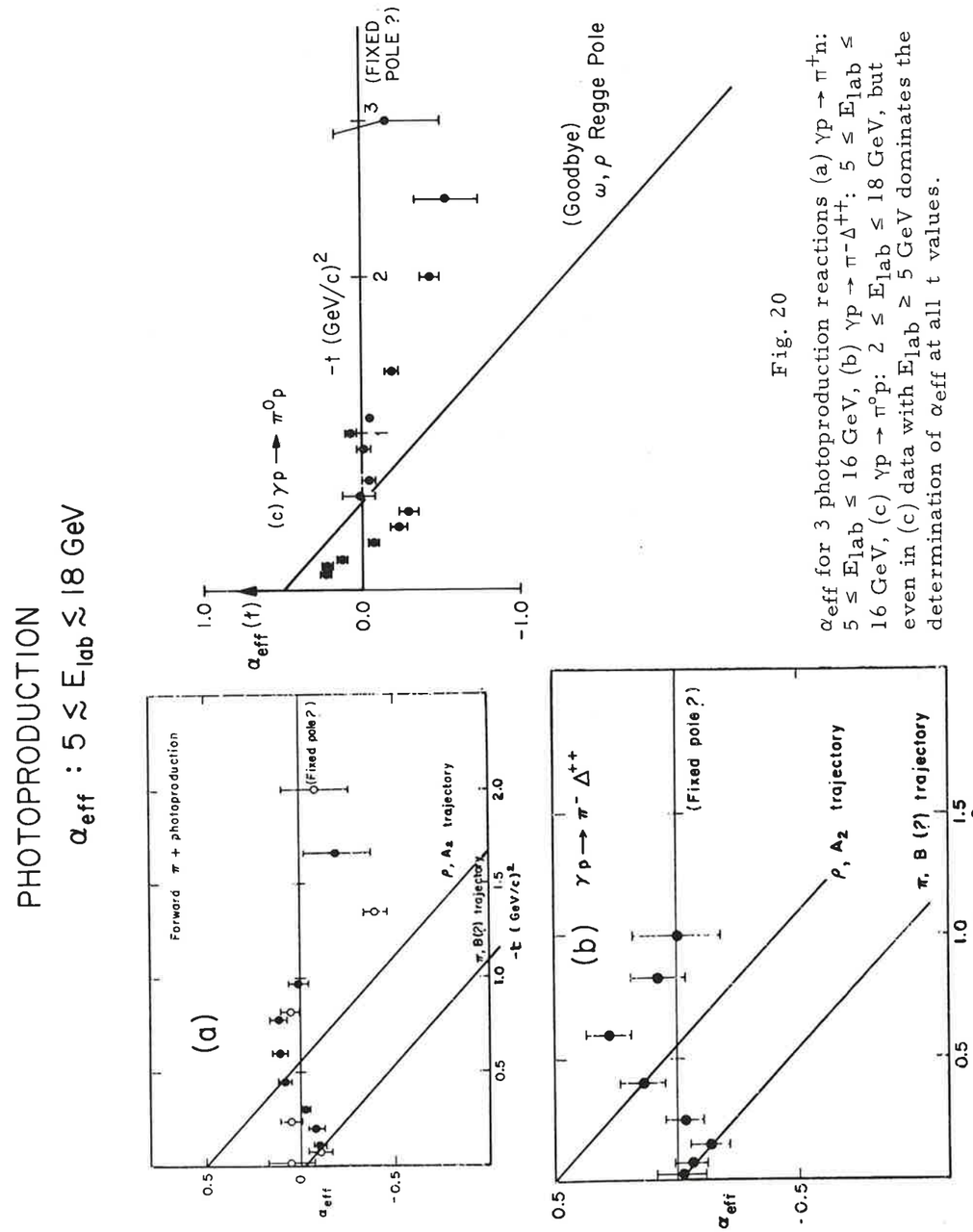

Fig. 20

α_{eff} for 3 photoproduction reactions (a) $\gamma p \to \pi^+ n$: $5 \le E_{lab} \le 16$ GeV, (b) $\gamma p \to \pi^- \Delta^{++}$: $5 \le E_{lab} \le 16$ GeV, (c) $\gamma p \to \pi^0 p$: $2 \le E_{lab} \le 18$ GeV, but even in (c) data with $E_{lab} \ge 5$ GeV dominates the determination of α_{eff} at all t values.

STRONG INTERACTIONS

α_{eff} : $2 \lesssim P_{lab} \lesssim 5$ GeV/c

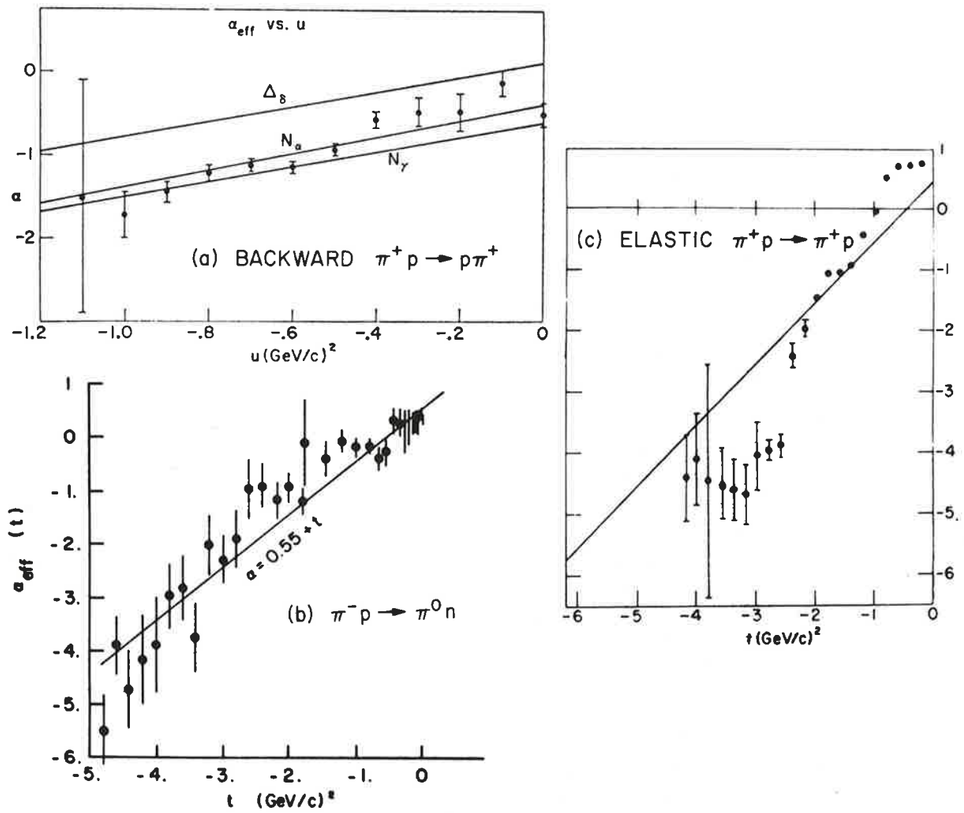

Fig. 21. α_{eff} for 3 strong interaction experiments (a) backward $\pi^+ p \rightarrow p\pi^+$: $3.25 \leq p_{lab} \leq 5.25$ GeV/c (Ref. 35), (b) $\pi^- p \rightarrow \pi^0 n$: $2 \leq p_{lab} \leq 5$ GeV/c (Ref. 36), (c) forward $\pi^+ p \rightarrow p\pi^+$: $2.5 \leq p_{lab} \leq 16.7$ GeV/c (Ref. 37), but even in (c) all the points in large $-t > 1$ (GeV/c)^2 come from $2.5 \leq p_{lab} \leq 5$ GeV/c.

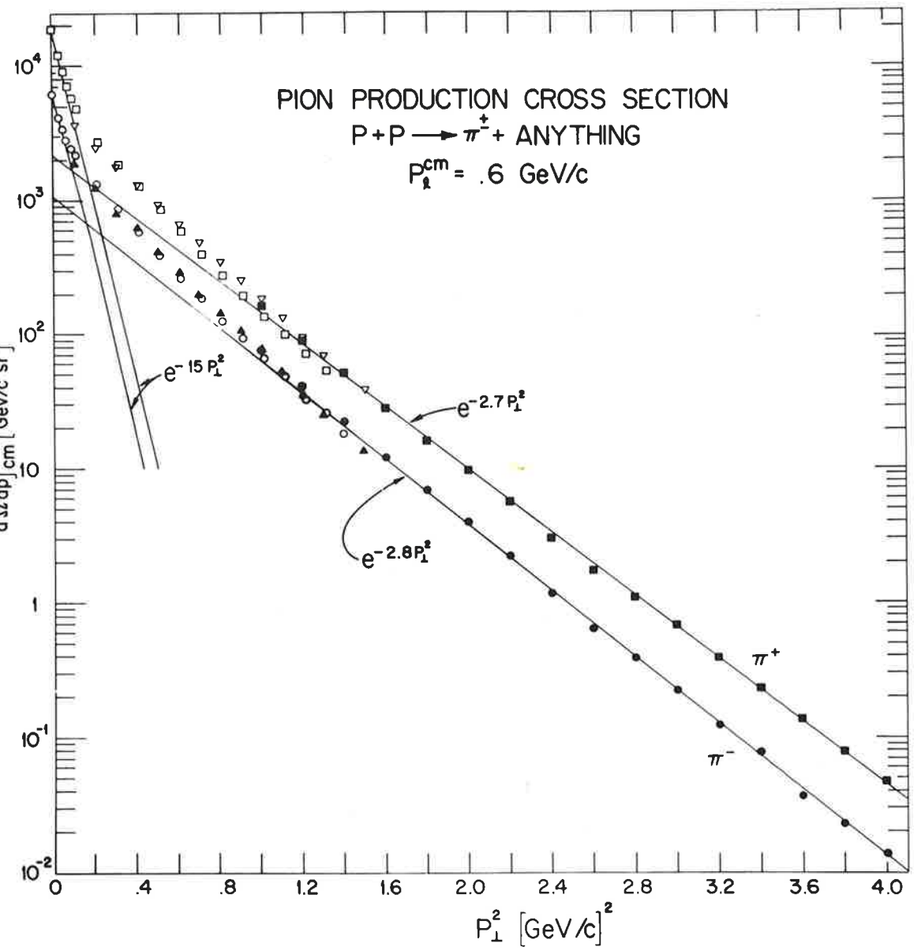

Fig. 22. Plot of $d^2\sigma/d\Omega\, dp$ v. $p_\perp^2$ for the inclusive reaction $pp \rightarrow \pi^\pm$ plus anything at 12.5 GeV/c (Ref. 41). $p_\perp$ is the component of the pion momentum transverse to the incident beam direction while the longitudinal momentum p_L of the π in the c.m.s. is held fixed at 0.6 GeV/c. The exponential fits show the same $e^{\simeq -3 p_\perp^2}$ behavior of large -t two-body data. (Remember in this latter case $-t \simeq p_\perp^2$.)